**IZMIR KATIP CELEBI UNIVERSITY**

**GRADUATE SCHOOL OF NATURAL AND APPLIED SCIENCES**

# FINITE ELEMENT ANALYSIS OF MATERIAL AND PARAMETER EFFECTS IN BALLISTIC ARMORS

**M.Sc. THESIS**

**Latif Tibet AKTAŞ**

**Department of Mechanical Engineering**

**Thesis Advisor: Assoc. Prof. Dr. Mehmet ÇEVİK**

**JULY 2018**

**IZMIR KATIP CELEBI UNIVERSITY**

**GRADUATE SCHOOL OF NATURAL AND APPLIED SCIENCES**

**FINITE ELEMENT ANALYSIS OF MATERIAL AND PARAMETER EFFECTS IN BALLISTIC ARMORS**

**M.Sc. THESIS**

**Latif Tibet AKTAŞ**
**(Y160217005)**

**Department of Mechanical Engineering**

**Thesis Advisor: Assoc. Prof. Dr. Mehmet ÇEVİK**

**JULY 2018**

**İZMİR KATİP ÇELEBİ ÜNİVERSİTESİ**
**FEN BİLİMLERİ ENSTİTÜSÜ**

**BALİSTİK ZIRHLARDA MALZEME VE PARAMETRE ETKİLERİNİN**
**SONLU ELEMANLAR YÖNTEMİYLE ANALİZİ**

**YÜKSEK LİSANS TEZİ**

**Latif Tibet AKTAŞ**
**(Y160217005)**

**Makine Mühendisliği Ana Bilim Dalı**

**Tez Danışmanı: Doç. Dr. Mehmet ÇEVİK**

**TEMMUZ 2018**

Latif Tibet AKTAŞ, a **M.Sc.** student of **IKCU Graduate School Of Natural And Applied Sciences**, successfully defended the thesis entitled "**FINITE ELEMENT ANALYSIS OF MATERIAL AND PARAMETER EFFECTS IN BALLISTIC ARMORS**", which he prepared after fulfilling the requirements specified in the associated legislations, before the jury whose signatures are below.

**Thesis Advisor :**

      **Assoc. Prof. Dr. Mehmet ÇEVİK** .........................
İzmir Katip Çelebi University

**Jury Members :**

      **Prof. Dr. Buket OKUTAN BABA** ........................
İzmir Katip Çelebi University

      **Assist. Prof. Dr. Gözde SARI** ........................
Manisa Celal Bayar University

**Date of Submission  : 12.06.2018**
**Date of Defense        : 03.07.2018**

*To my family,*

**FOREWORD**

I would like to thank my advisor, Assoc. Prof. Dr. Mehmet ÇEVİK, for all the support and excellent guidance he provided to me.

Thanks to Prof. Dr. Buket OKUTAN BABA and Asst. Prof. Dr. Levent AYDIN, for preparing me to become a Master of Science.

Finally, my grateful thanks to my family who encouraged me and supported me along the way.

July 2018                                                                 Latif Tibet AKTAŞ

# TABLE OF CONTENTS

## ABBREVIATIONS

| | |
|---|---|
| **UHMWPE** | : Ultra High Molecular Weight Polyethylene |
| **FE** | : Finite Element |
| **CFRP** | : Carbon Fiber Reinforced Polymer |
| **FGM** | : Functionally Graded Material |
| **FMJ** | : Full Metal Jacket |
| **ANSI** | : American National Standards Institute |
| **SAAMI** | : Sporting Arms and Ammunition Manufacturers Institute |
| **CNT** | : Carbon Nanotube |

# LIST OF TABLES

# LIST OF FIGURES

# FINITE ELEMENT ANALYSIS OF MATERIAL AND PARAMETER EFFECTS IN BALLISTIC ARMORS

## ABSTRACT

Bulletproof composite armor models are investigated using finite element software ANSYS/AUTODYN. A composite plate is modelled with Kevlar 29/epoxy, analysed, and the results obtained by this model are confirmed with the results available in the literature. Different materials are tested as secondary materials in the composite plate. The results obtained by these materials for unit weight and for residual velocities of the projectile are compared. A new stacking sequence study is conducted with the Kevlar 29/epoxy as primary material and Ultra High Molecular Weight Polyethylene (UHMWPE) as secondary material. Four different stacking sequences are tested considering the absorbed kinetic energy of the projectile. A final composite plate is modelled using the stacking sequence with the best kinetic energy absorption rate and UHMWPE as the secondary material. Investigation of material effects on high velocity impact loading indicates that this final plate model consisting of Kevlar 29/epoxy - UHMWPE layers is lighter and more successful at decelerating the bullet velocity than a plate consisting of only of Kevlar 29/epoxy layers. Finally, high velocity impact tests on the model with different projectile velocities, different shapes of projectile and target plate, a standard bullet model and different impact angles are conducted and the results with residual velocities of the bullet and kinetic energies absorbed by the plate are compared.

# BALİSTİK ZIRHLARDA MALZEME VE PARAMETRE ETKİLERİNİN SONLU ELEMANLAR YÖNTEMİYLE ANALİZİ

## ÖZET

Bu çalışmada kurşungeçirmez kompozit zırh modelleri, ANSYS/AUTODYN sonlu elemanlar yazılımı kullanılarak incelenmiştir. Kevlar 29/epoksi içeren bir plaka modellenmiş, analiz edilmiş ve elde edilen sonuçlar literatürdeki sonuçlarla karşılaştırılarak modelin doğrulaması yapılmıştır. Ardından ikincil malzeme olarak kullanılmak üzere farklı malzemeler test edilmiş ve test sonuçları birim ağırlık ve mermi artık hızı cinsinden karşılaştırılmıştır. Kevlar 29/epoksi'nin yanında ikincil malzeme olarak Ultra Yüksek Moleküler Ağırlıklı Polietilen (UYMAPE) kullanılarak tabaka dizilimi çalışması yürütülmüştür. Merminin plaka tarafından sönümlenen kinetik enerjisi ölçülerek dört farklı tabaka dizilimi analiz edilmiştir. Bu dizilimler arasından enerji sönümleme kabiliyeti en yüksek olan seçilmiş ve ikincil malzeme olarak UYMAPE kullanılarak nihai bir kompozit plaka modeli geliştirilmiştir. Bu nihai modelin, literatürden seçilen ve sadece Kevlar 29/epoksi'den oluşan plakaya göre daha hafif ve mermiyi yavaşlatmada daha etkili olduğu gözlemlenmiştir. Son olarak yeni model üzerinde farklı mermi hızları, farklı mermi ve plaka şekilleri, seçilen bir standart mermi modeli ve farklı çarpma açıları kullanılarak yüksek hızlı çarpışma testleri yapılmış, mermi artık hızı ve plaka tarafından sönümlenen kinetik enerji miktarı sonuçları karşılaştırılarak sunulmuştur.

# 1. INTRODUCTION

The technology of composite materials is based on combining two or more different materials in one system and taking advantages of each material component in that system. Composites are very important materials in defense applications, especially in production of bulletproof systems. In battlefield or in minor operations, personal armors with bulletproof systems are the final frontier of protection against projectile impact. Bulletproof composites are used in covering the most important body parts as in helmets, vests and shields. Despite all the advantages of composite armors like mobility and lightness, they still need to be improved because their protection efficiencies against high-velocity projectile impact are not perfect. Even when the impact energy is almost absorbed and the contact of projectile with the protected asset is blocked, the residual impact energy transferred to the protected surface is still high and should be decreased.

Improvement of composite ballistic armors depends on various parameters and their combined effects on strength properties.

Varas et al. [1] studied carbon-epoxy composite laminates and observed residual velocities of projectiles at different impact velocities. They did numerical simulations using ABAQUS finite element (FE) software and performed experimental tests for the validation of their model.

Zhang et al. [2] investigated material effect on high-velocity impact response of Al alloy targets. They validated their computer simulations with experiments and concluded that Al-Sc alloys demonstrate more resistance to high-velocity impacts than Al-Ti alloys.

Mohotti et al. [3], studied high-velocity ballistic impacts on polyurea coated aluminum plates. They suggested an analytical model and validated this model experimentally and numerically. The influence of polyurea coating on ballistic strength was investigated and it was shown that the polyurea coated plates showed lower deformation compared to the uncoated plates.

Park et al. [4], compared kinetic energy absorption properties of pure Kevlar and Kevlar plates impregnated with shear thickening fluid. After experimental and

numerical high-velocity impact tests, they deduced that impregnated Kevlar plates absorb more impact energy than neat Kevlar plates. In addition, they showed that 8 layers of pure Kevlar and 5 layers of Kevlar impregnated with shear thickening fluid absorbed almost the same magnitude of impact energy.

López-Puente et al. [5] studied the failure development in the laminate with the help of C-scan and compared numerical simulation results that were obtained by using the commercial FE code ABAQUS and mathematics code MATLAB with experimental results. MATLAB software was used to calculate the damaged area on woven CFRP laminates in this study. The same team [6] also used a numerical FE model for woven carbon/epoxy laminates to investigate residual velocity of projectile and damaged region that occurred after high velocity impacts. They concluded that the ballistic limit of plate depends on the angle of impact but this angle does not affect the residual velocity once the ballistic limit is exceeded.

Bland & Dear [7] observed connection time of projectile and target, bending and perforation of impact zone on the target, residual impact energy and failure parameters of impact experiments on carbon-fiber reinforced polymers. They focused on two different extreme impact conditions of high speed/low weight and low speed/high weight.

Hammond et al. [8] studied impact response of carbon-fiber reinforced polymer composites with different stacking forms (quasi-isotropic and uni-directional) using high-speed optical techniques. They experimentally studied damage patterns on the plates in macro scale and micro scale.

Hosur et al. [9] experimented high velocity impact response of carbon/epoxy woven composites. Their intention was to determine the effects of stitching layers and the experiments were done for different number of layers. It was observed that stitched laminates contain the damage propagation well within the grid structure but unstitched laminates showed higher ballistic limit behavior.

Kim et al. [10] studied impact effects of spherical shaped simulated hail ice on carbon/epoxy woven plates. They focused on determining the failure resistance of composite structures with small thickness to ice impact. Different parameters like material, lay-up sequence, plate thickness and their effects on woven formed

carbon/epoxy composite plates were tested in layered and monolithic forms of composite plates.

Cantwell & Morton [11] conducted studies on CFRP laminates to study impact responses of composite systems under low and high velocity impact loading conditions. They found that under low velocity impact loading, it is the structural geometry that determines impact response of the target. On the other hand, effects of dimensional measurements like width and length of the plate had little influence on the impact response under high velocity impact loading condition in their experiments.

Will et al. [12] investigated projectile impact loading on CFRP filament wound tubes and the effects of laminate stacking sequence. They experimented energy dissipations of two different lay-up sequences and performed a static FE analysis using ABAQUS code.

Tham et al. [13] presented the results of comparison between experiments and simulations on ballistic impacts of Kevlar helmet. Their experiment included high speed velocity impact loading on a Kevlar helmet with spherical projectile. The AUTODYN-3D simulation results were in good agreement with their experiment. They included different ballistic test standards and their simulations for Kevlar helmets in their paper. One of their conclusions was that Kevlar helmet could stop a 9 mm full metal-jacketed projectile with a speed of 358 m/s.

Garcia-Avila et al. [14] manufactured high-performance light-weight composite armor system using different materials and different manufacturing methods and evaluated the ballistic tolerance of this composite armor system. They performed finite element analysis to study failure mechanisms and energy absorption of the plate.

Min et al. [15] studied effect of reinforcement continuity on ballistic performance of composites made from multiply plain weave fabric. After producing continuous and discontinuous plain weave fabrics, they examined the damage morphology and confirmed the superiority of the continuously reinforced composites.

Wicklein et al. [16] derivated and validated of a numerical material model that predicts the highly dynamic behavior of CFRP under high velocity impact. Additionally, they compared the numeraically predicted damage within the CFRP to the delamination areas found in ultrasonic scans.

Zhou et al. [17] used FE models to predict the response of woven fabrics wiith different structural parameters. They confirmed that the plain woven fabric shows superior energy absorption over other structures in a aballistic event.

Rizov [18] investigated low velocity impact behavior of two densities of ductile polyvinylchloride foam and post-impact creep response of this foam. He studied development of a damage tolerance design approach for structural foams.

Toqueboeuf et al. [19] conducted dynamic compressive tests in different configurations and they found that the initial multi-axial prestress of polyurethane is one of the most important parameters for material and layered response.

Deka et al. [20] investigated the response of laminated composites subjected to high velocity, multi-site impacts from a modeling and experimental viewpoint. They compared energy absorption, new surface creation and failure mechanisms from sequential and simultaneous multi-site high velocity impacts.

Ansari & Chakrabarti [21] studied numerically on a validated model. The model consisted of 19 layers of Kevlar 29 and it was impacted by blunt nosed steel projectile. The impact velocity gap was from 25 m/s to 1000 m/s and they compared residual velocities of projectile as results. In addition, the ballistic limit variation, residual velocity of projectile, failure propagation in the impacted plate and in the projectile, penetration depth, kinetic energy of the projectile, deflection and radius of damaged zone were investigated.

The literature review reveals that most of the ballistic studies are focused on 2 or 3 different parameter effects. In this study, it is intended to find and compare the effects of specific materials on protection of composite ballistic armor plates against high-velocity projectile impact. In addition, the effects of stacking sequence for different materials, projectile type, target plate shape and impact obliquity are investigated individually. Ballistic limits and residual velocities are found and used for comparisations. Ballistic limit is a velocity value for a specific projectile to penetrate a plate at least 50% of the impact tests. Residual velocity is the velocity value of a projectile after leaving the perforated plate by itself. In order to get comparable results, one of the published studies [21] about this topic is chosen to verify the simulation. ANSYS/AUTODYN solver is used for modelling, numerical study and simulations.

## 2. NUMERICAL MODELLING AND METHOD

### 2.1 Material Properties

In the present study, the materials which are commonly used or are considered for possible use in impact applications have been tested. The aim was to investigate the effects of different material combinations as well as the velocity of projectile on composite ballistic armors. Dimensions of Steel 4340 projectile and Kevlar 29/epoxy armor plate, velocity of projectile, thickness and number of layers and material properties, which have been used in the present study were described in literature [13, 21, 22]. In Table 2.1, mechanical properties of Kevlar 29/epoxy are presented. Mechanical properties of Steel 4340 are shown in Table 2.2.

**Table 2.1 :** Mechanical properties of Kevlar 29/epoxy [21].

| | | | |
|---|---|---|---|
| Density (g/cm$^3$) | 1,65 | Tensile strength X (kPa) | 1,8500E+006 |
| Elastic modulus Z (kPa) | 1,9480E+006 | Tensile strength Y (kPa) | 1,8500E+006 |
| Elastic modulus X (kPa) | 1,7989E+007 | Shear strength XZ (kPa) | 5,4300E+005 |
| Elastic modulus Y (kPa) | 1,7989E+007 | Shear strength XY (kPa) | 7,7000E+004 |
| Poisson's ratio XZ | 0,0800 | Shear strength YZ (kPa) | 5,4300E+005 |
| Poisson's ratio XY | 0,0756 | Tensile failure strain Z | 0,0200 |
| Poisson's ratio YZ | 0,6980 | Tensile failure strain X | 0,0600 |
| Shear modulus XZ (kPa) | 2,2300E+005 | Tensile failure strain Y | 0,0600 |
| Shear modulus XY (kPa) | 1,8570E+006 | Max. shear strain XZ | 1,0000E+020 |
| Shear modulus YZ (kPa) | 2,2300E+005 | Max. shear strain XY | 1,0100E+020 |
| Tensile strength Z (kPa) | 1,2000E+006 | Max. shear strain YZ | 1,0100E+020 |

**Table 2.2 :** Mechanical properties of Steel 4340 [21].

| | | | |
|---|---|---|---|
| Equation of states | Linear | Hardening constant (kPa) | 5,1000E+05 |
| Density (g/cm$^3$) | 7,8300 | Hardening exponent | 0,26 |
| Bulk modulus (kPa) | 1,5900E+08 | Strain rate constant | 0,0140 |
| Strength | Johnson – Cook | Thermal softening exponent | 1,0300 |
| Shear modulus (kPa) | 7,7000E+07 | Melting temperature (K) | 1793 |
| Yield stress (kPa) | 7,9200E+05 | Failure | Johnson – Cook |

Johnson & Cook [23] presented a material model about the relationship between strain rate, strain hardening and thermal softening and the model is described in equation (2.1).

$$\sigma = (A + B\varepsilon^n)\left(1 + C\ln\left(\frac{\dot{\varepsilon_p}}{\dot{\varepsilon_0}}\right)\right)(1 - T^{*m}) \qquad (2.1)$$

The $\varepsilon^* = \dot{\varepsilon_p}/\dot{\varepsilon_0}$ expression is dimensionless plastic strain rate where $\dot{\varepsilon_0} = 1.0$ s$^{-1}$. A, B, n, C and m are material constants and T$^*$ is the homologous temperature. Homologous temperature states the temperature of a material as a fraction of its melting point temperature. The expression in the first brackets gives the stress as a function of strain. The expressions in the second bracket gives the effect of strain rate and for the third bracket, it gives the effect of temperature [23].

## 2.2 FE Model of the Target Plate and the Projectile

ANSYS/AUTODYN v15.0 engineering design and 3-D simulation software is used for modelling, simulation and analysis of composite plate and projectile. It is one of the most preferred FE software in the academic studies which focused on numerical investigation of explicit dynamics. Explicit dynamics is one of the analysis modules in ANSYS Workbench that specialized on solving problems about short duration and high pressure loading impacts, i.e. dynamic analyses. It is qualified for analysing ballistic impact scenarios.

As a FE software, ANSYS uses different element types. For the ballistic plate modelling in ANSYS, shell and plane elements are used generally. Shell elements are

used for thin structures where one dimension significantly smaller than the other dimensions, that is, they are plane stress elements and can be used for curved structures. On the other hand, plane elements are used for other basic FE analyses that the element has significant dimensions in every axis. For the present study, since the elements of the ballistic plate have no insignificant dimension, plane elements are used in the FE software. The two fundamental structural solid plane element types of ANSYS are PLANE-182 and PLANE-183. These two element types can be used in plane stress and plane strain conditions. PLANE-182 is defined by four nodes and each node has two degrees of freedom, as shown in Figure 2.1. PLANE-182 element has plasticity, hyperelasticity, stress stiffening, large deflection and large strain capabilities [24]. PLANE-183 is an 8 or 6 nodes element, depending on the element shape, as shown in Figure 2.2. PLANE-183 element has creep capability besides all the capabilities of PLANE-182 element [18]. In fact, when the midside nodes of PLANE-183 element are dropped, then it becomes PLANE-182 element. However, element midside nodes must be dropped for Explicit Dynamics module. Thus, PLANE-183 element can not be used for Explicit Dynamics. The midside node differences can be seen in Figure 2.3.
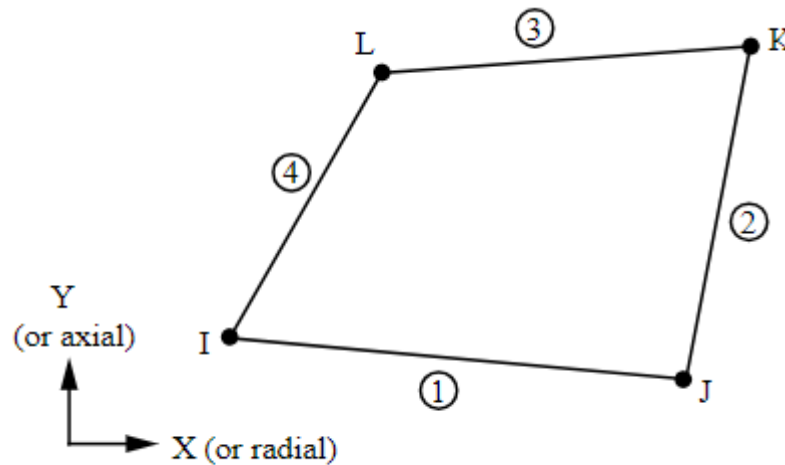


**Figure 2.1 :** PLANE-182 element geometry [24].
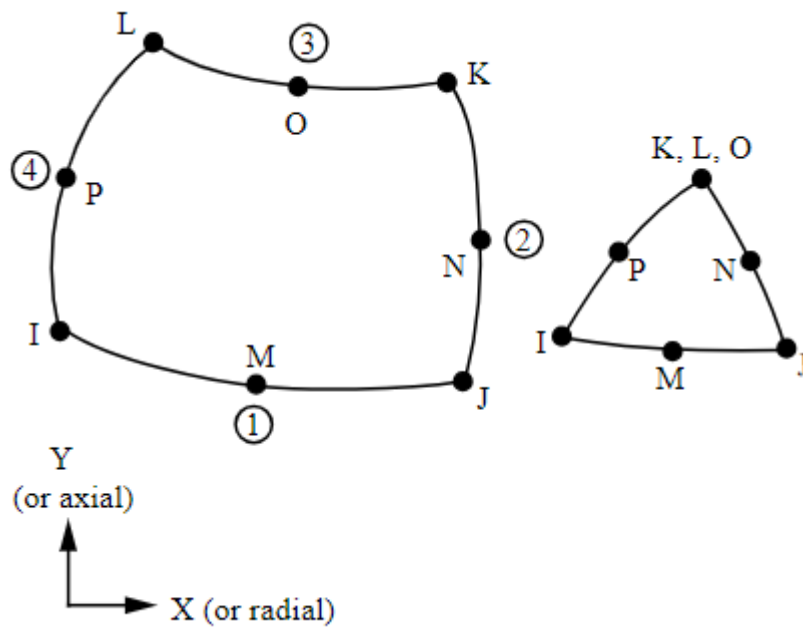
**Figure 2.2 :** PLANE-183 element geometry [25].
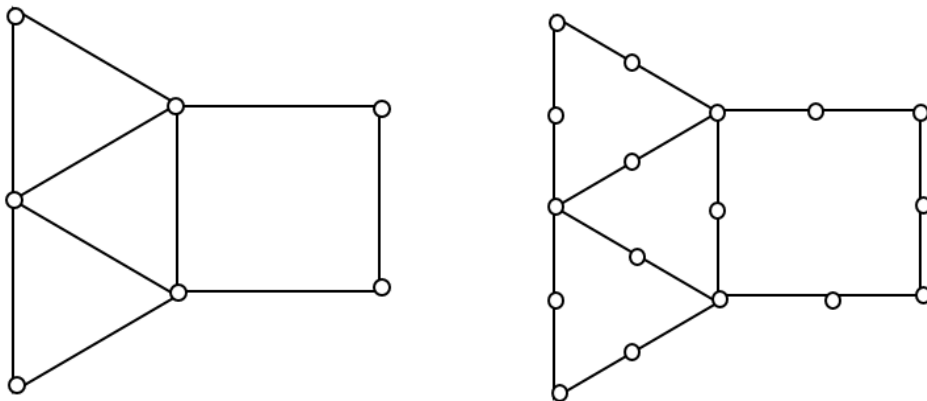


**Figure 2.3 :** Element midside nodes illustrations for dropped (left) and kept (right).

## 2.3 Verification of the FE Model

The applicability and the accuracy of the present FE model is validated by comparing our results with those of Ansari & Chakrabarti [21]. The present study provides results in good agreement with their results, as seen in Table 2.3. The negativity in velocities represents failure of full penetration of the plate and recoil motion of the projectile. After calibrating the software options and validating the results, effects of different

parameters could be tested and their results can be accepted as reliable. As a result, it can be concluded that the numerical results of the present study are close to the results of Ansari & Chakrabarti [21].

**Table 2.3 :** Comparison of present impact results with those of [21].

| Impact velocity (m/s) | Residual velocity (m/s) [21] | Residual velocity (m/s) (present study) |
|:---:|:---:|:---:|
| 200 | -48,93 | -48,64 |
| 300 | -44,72 | -38,4 |
| 500 | 267,24 | 265,49 |
| 650 | 442,1 | 431,38 |
| 850 | 670,5 | 629,17 |

In order to check the effect of modelling fraction on analysis process, an aluminum circular plate of radius 25 mm and thickness of 2,5 mm is modelled. The projectile has a lead core and copper jacket. The radius of the projectile is 4,5 mm, mass of the projectile 5 grams and its impact velocity is 500 m/s. The boundary conditions are all-clamped for the plate. Mesh convergence visual of the model is shown in Figure 2.4. Equivalent stress results and the visual of the penetration is shown in Figure 2.5.
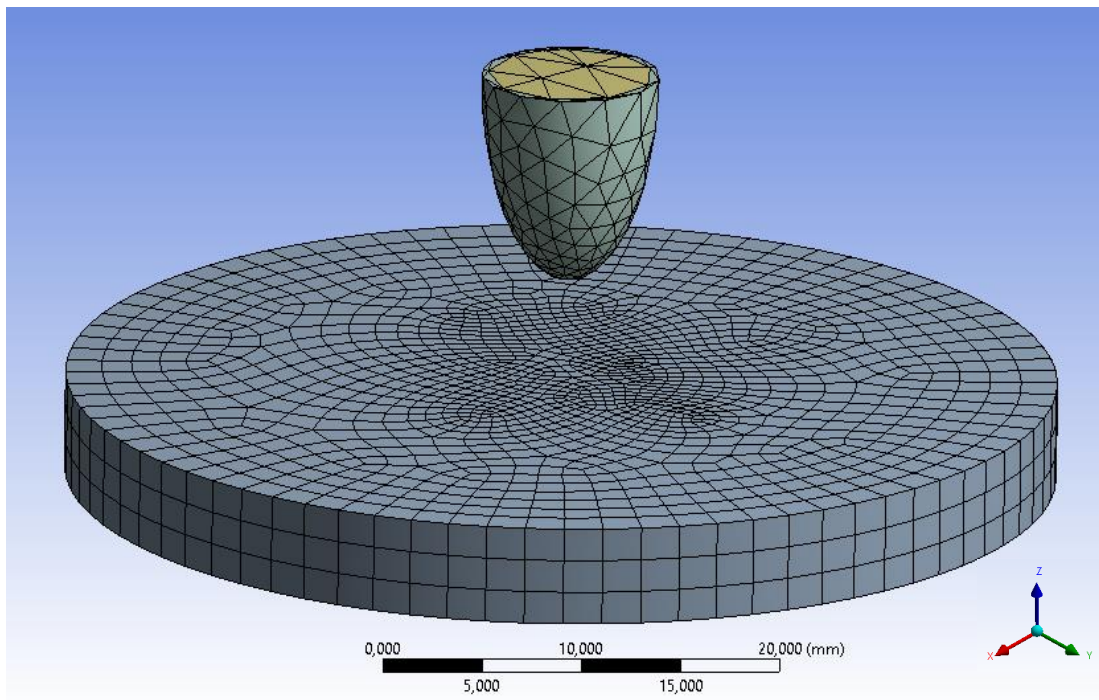


**Figure 2.4 :** Full plate and projectile model and their mesh convergence.
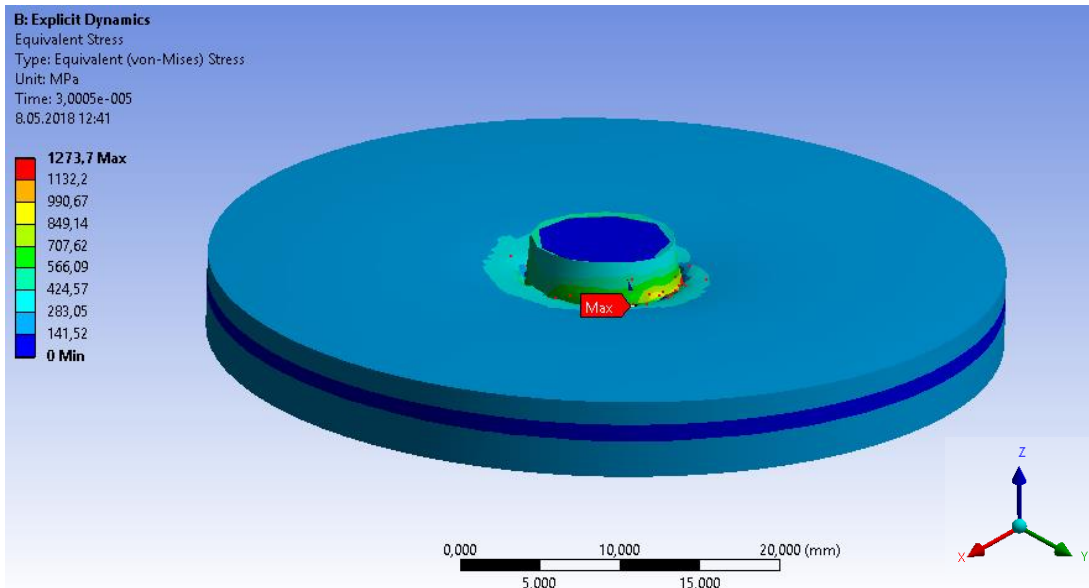
**Figure 2.5 :** Equivalent stress results for full plate and projectile model.

To simplify the analyzing process and to shorten the calculation time, 1/4 fraction of the same plate is modelled. For 1/4 fraction of the model, the base surfaces of the plate and the projectile are revolved 90° about the axisymmetry axis. Symmetrical boundary conditions are defined for the cutting lines of the models to compare quarter model to full one. Mesh convergence visual of the 1/4 model is shown in Figure 2.6.
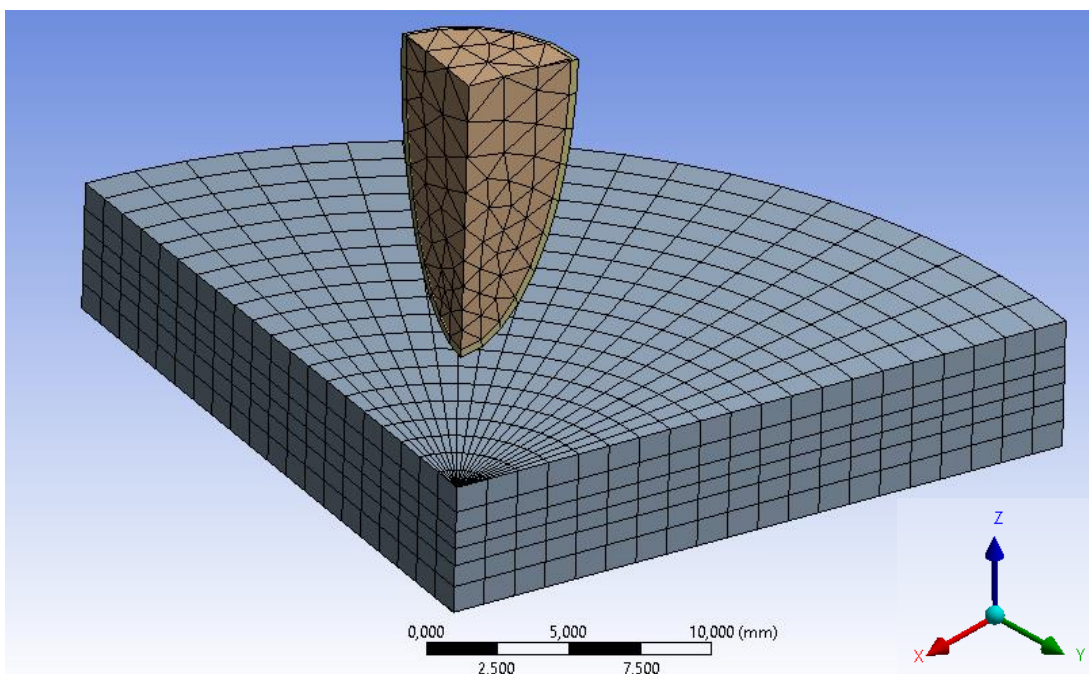


**Figure 2.6 :** Quarter plate and projectile model and their mesh convergence.

An equivalent stress analysis is conducted by focusing on the center of the plate where the projectile impacted. Equivalent stress results and the visual of the penetration are shown in Figure 2.7. Comparison of the test results are shown in Table 2.4. After the stress analysis, considering the analysis time and approximation of results, it is concluded that one quarter model can be utilized for the rest of the study.
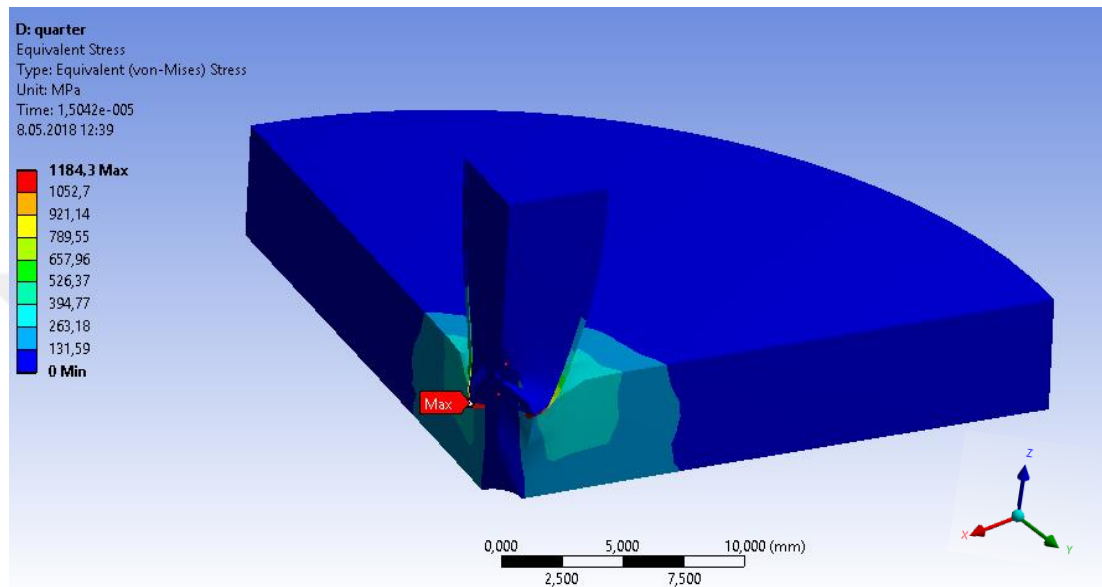


**Figure 2.7 :** Equivalent stress results for quarter plate and projectile model.

**Table 2.4 :** Comparison of equivalent stress simulation results and analysis time for modelled fraction of the plate.

| Modelled fraction of the plate | Maximum value of equivalent stress (GPa) | Analysis time (min) |
|---|---|---|
| 1/1 | 1,274 | 31 |
| 1/4 | 1,184 | 4,6 |

Literature review of ballistic impact studies shows that the most commonly used shape and boundary condition of target plate is rectangular plate with all-clamped boundary conditions [1, 4, 21]. In order to get comparable results, Ansari and Chakrabarti's study [21] is taken as a reference and modelling and testing processes started consistent with their study. For this purpose 19 layers of Kevlar 29/epoxy woven is modelled and stacked into one plate. Each layer has a thickness of 0,5 mm and total thickness of the plate is 9,5 mm. The plate is impacted by a flat nosed cylindrical Steel 4340 projectile which has an impact velocity of 500 m/s. The projectile is 10 mm in diameter and has a mass of 6,15 gr. The Kevlar 29/epoxy plate has a square shape with the dimensions

of 100 mm × 100 mm and the boundary conditions are all-clamped at all boundaries. The modelling has been done with a gap of 0,038 mm between the projectile and the plate which is the position just before the impact. Projectile movement parallel to the plate plane is constrained while its movement perpendicular to the plate plane is free. Since a quarter of the plate is modelled in three dimensions, symmetrical boundary conditions have been defined for the cutting lines. Connections between the layers are defined as bonded and between the projectile and laminate as frictionless.

Mesh refinement has been carried out non-uniformly. Finer meshing gives more realistic simulation results but it takes much more time of analysis. In order to get optimal meshing, a mesh convergence study is performed and it is seen that using fine mesh at the impact region and coarse mesh at the rest of the laminate where there is no loading, yields effective results and takes reasonably less analysis time than using uniform meshing. By the mesh convergence study trials, it is found that a mesh division of 15×15 with a bias factor of 7 shows good convergence when compared with the results of those available in the literature [21]. Bias factor is about rearranging mesh dimensions exponentially through one edge of a geometry. It is used for getting dense meshing at the position where the load concentration is applied on and obtain precise results from the position. Bias factor can be formulized as

$$L = \sum_{0}^{i} l1 \times r^i \qquad (2.2)$$

and

$$bf = r^{(n-1)} \qquad (2.3)$$

where L indicates edge length, r indicates growth rate, $l1$ indicates length of first mesh element and n indicates number of mesh divisions on edge. $i$ value can be in a range from 1 to $n-1$ [26].

Each layer is divided into 2 mesh slices along their thicknesses. The results of the mesh convergence studies under high velocity impact of 500 m/s are compared and have been presented in Table 2.5. First 3 rows in the table shows other trials to obtain

reliable resemblance between present study and control study [21]. Final meshing of the laminate is shown in Figure 2.8.

**Table 2.5 :** Comparison of impact simulation results for different element sizes.

| Number of elements by width × depth × height | Total number of elements for a quarter plate | Residual velocity of the projectile (m/s) |
|---|---|---|
| 30×30×19 | 17100 | 242,00 |
| 30×30×38 | 34200 | 275,28 |
| 20×20×38 | 15200 | 244,28 |
| 15×15×38 (Present study) | 8550 | 265,49 |
| 50×50×19 [21] | 47500 | 267,24 |
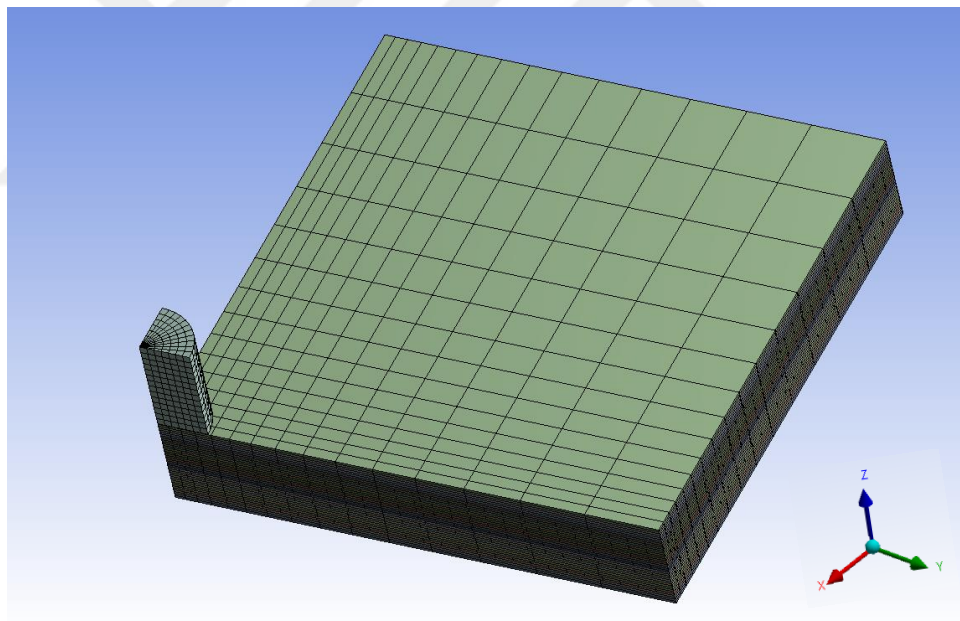


**Figure 2.8 :** Quarter rectangular plate and flat nosed cylindrical projectile with 15×15 mesh division.

## 2.4 Corrugated layered plate trial

In modelling sense, one of the innovative products designed and produced with special methods is corrugated Kevlar layers. The idea of corrugated layer model is reroute and

slow down the projectile with the help of grooves. The main parameter of these models is the angle of grooves, by changing the angles to reroute and/or slow down the projectile effectively.

Considering this type of model, a basic corrugated Kevlar 29/epoxy plate is modelled. There are 10 layers of Kevlar 29/epoxy and 3 of them are corrugated. Because of the greater thickness of corrugated layers, the 10 layered model has the same thickness with the 19 layered previous model. The corrugated Kevlar 29/epoxy model is shown in Figure 2.9.
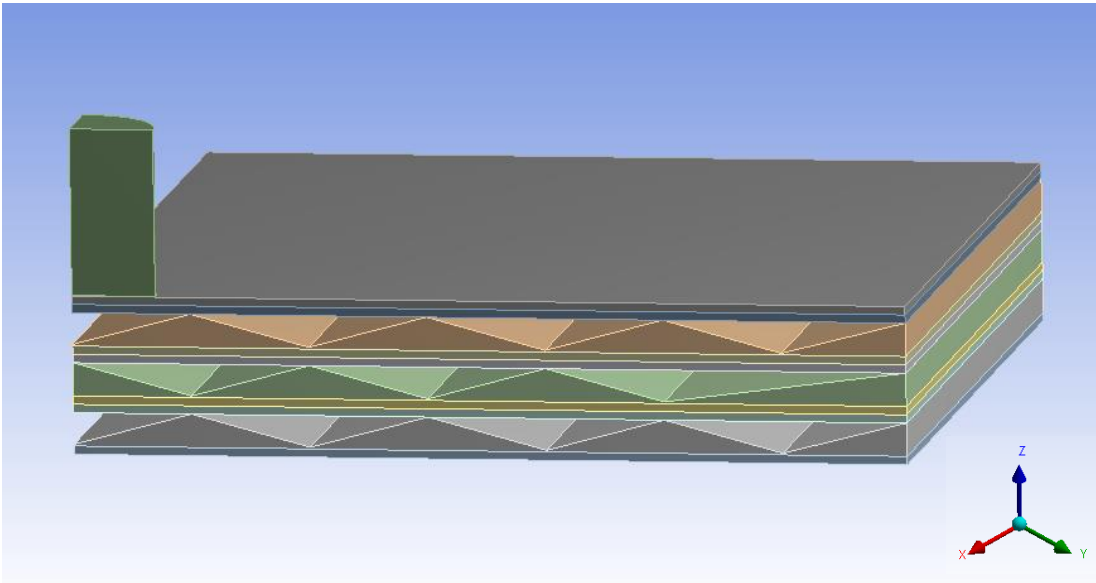


**Figure 2.9 :** Corrugated Kevlar 29/epoxy plate model.

The test indicates that 7 layers of normal and 3 layers of corrugated Kevlar 29/epoxy plate decelerates the velocity of identical Steel 4340 projectile inadequately than 19 layers of normal Kevlar 29/epoxy plate. However, this cannot indicate the exact comparison between normal and corrugated plates considering the basic modelling of the corrugated plate and lack of secondary material placed in the voids of the grooves. The basic comparison between normal and corrugated Kevlar 29/epoxy plates is shown in Table 2.6.

**Table 2.6 :** Comparison of impact simulation results for normal and corrugated Kevlar 29/epoxy plates.

| Type of Kevlar 29/epoxy plate | Total weight of the plate* (g) | Residual velocity of the projectile (m/s) |
|---|---|---|
| Normal | 156,750 | 265,49 |
| Corrugated | 109,710 | 369,96 |

* The weight of 100×100 mm plate

## 2.5 Graphene film covering trial

Graphene is a sheet of carbon atoms bonded as honeycomb shape. This relatively new material is well known for its high strength. Thus, a thin layer of graphene film is modelled to cover the 19 layered Kevlar 29/epoxy plate. The minimum layer thickness limit of ANSYS Workbench is 30 nm and even though this thickness value is enough to model one sheet of graphene, the analysis could not be done because of the insufficient processor power. Impact tests of plates covered with graphene films require superior processor power because of the combined analysis of macro and nano scales together in one model.

Carbon nanotubes (CNTs) are the cylindrical form of graphene sheets. The major difference between CNT and graphene is the greater thickness of CNTs than graphene because of its cylindrical form. However, the analysis could not be done despite the increased thickness of CNT layer.

# 3. RESULTS AND DISCUSSION

## 3.1 Effect of Material on Ballistic Response

In this section, residual velocity of a flat nosed Steel 4340 projectile is investigated depending on different target plate component materials. The effect of these materials on total plate weight is examined. Boundary conditions of the plate are always all-clamped. The number and thickness of layers of the composite plate have been kept constant in order to observe the effect of different component materials. Same dimensions are used for the plate, 100 × 100 mm; and same impactt velocity is used as 500 m/s for projectile. For this purpose, 6 major materials are focused on which are being commonly used in academic and commercial applications of ballistic armors. It is known that one of these materials, Kevlar 29/epoxy, has superior ballistic properties; and thus, each of the other five materials is accompanied with Kevlar 29/epoxy layers. The layers have been stacked in such a sequence that 9 layers of each 5 test materials are placed in between 10 Kevlar 29/epoxy layers. The layer stacking sequence notation can be expressed as $[(K/X)_9/K]$, where K indicates Kevlar 29/epoxy and X indicates the material which accompanies with Kevlar 29/epoxy. Each layer of both Kevlar 29/epoxy and test material is designed with the same thickness of 0.5 mm as woven ply. Residual velocity test results of flat nosed cylindrical Steel 4340 projectile for different secondary materials of rectangular target plate are shown in Table 3.1. Pure Kevlar 29/epoxy means 19 layers of Kevlar 29/epoxy plate and the other materials indicate 9 layers of mentioned material accompanied with 10 layers of Kevlar 29/epoxy.

**Table 3.1 :** Residual velocities of flat nosed cylindrical projectile for different secondary materials of target plate.

| Material | Layer weight (g) | Total weight of the plate* (g) | Residual velocity (m/s) |
|---|---|---|---|
| Pure Kevlar 29/epoxy | 8,250 | 156,750 | 265,490 |
| H100 foam | 0,500 | 87,000 | 360,000 |
| Polyurethane | 6,325 | 139,426 | 330,180 |
| UHMWPE | 4,850 | 126,150 | 300,600 |
| Graphite | 11,250 | 183,750 | 299,280 |
| S2 Glass | 9,250 | 165,750 | 316,380 |

Analysis of material effects on high velocity impact loading indicates that heavier plates do not necessarily provide higher protection against high velocity impacts. As shown in Table 3.1, Kevlar 29/epoxy plate itself absorbs more kinetic energy of projectile than its heavier competitor, graphite, and lets the projectile exit with a lower velocity. On the other hand, H100 foam is a much lighter material, yet the exit velocity of the projectile from Kevlar 29/epoxy – H100 foam plate is much higher than from others. Comparison of the two popular polymers shows that UHMWPE (Ultra High Molecular Weight Polyethylene) is better at kinetic energy absorption of high velocity projectile than polyurethane, even polyurethane is heavier than UHMWPE. Considering the full layer weight, H100 foam is lighter than UHMWPE; however, the residual velocity of the projectile tested on H100 foam is approximately 19,26% faster than the one tested on UHMWPE. In the terms of ballistic strength of material, graphite is 0,86% better at slowing down the projectile than UHMWPE but considering their unit layer weights, UHMWPE is 56,88% lighter than graphite. Kevlar 29/epoxy – UHMWPE composite plate demonstrates poor kinetic energy absorption than pure Kevlar 29/epoxy plate itself but in the terms of getting lighter composite plate, Kevlar 29/epoxy – UHMWPE composite is focused on in this study. Material properties of UHMWPE described in literature are used in the present FE simulation and these properties are shown in Table 3.6 [27].

**Table 3.2 :** Material properties of one layer of H100 Foam [18].

| Density (kg/m$^3$) | Young's modulus (MPa) | Shear modulus (MPa) | Poisson's ratio | Compressive strength (MPa) |
|---|---|---|---|---|
| 100 | 125 | 48 | 0,31 | 1,7 |

**Table 3.3 :** Material properties of one layer of Polyurethane [19].

| Density (kg/m$^3$) | Young's modulus (MPa) | Shear modulus (MPa) | Poisson's ratio | Bulk modulus (GPa) |
|---|---|---|---|---|
| 1190 | 4 | 5 | 0,48 | 2 |

**Table 3.4 :** Material properties of one layer of Graphite [29].

| Density (kg/m$^3$) | Young's modulus (GPa) | Compressive strength (MPa) | Flexural strength (MPa) |
|---|---|---|---|
| 1600 | 10 | 100 | 50 |

**Table 3.5 :** Material properties of one layer of S2 Glass [20].

| Tensile modulus (GPa) | | | Density (g/cm$^3$) | | |
|---|---|---|---|---|---|
| $E_z$ | $E_x$ | $E_y$ | | | |
| 12 | 27,1 | 27,1 | 1,85 | | |

| Shear modulus (GPa) | | | Poisson's ratio | | |
|---|---|---|---|---|---|
| $G_{xz}$ | $G_{yz}$ | $G_{xy}$ | $\nu_{xy}$ | $\nu_{yz}$ | $\nu_{xy}$ |
| 2,14 | 2,14 | 2,9 | 0,11 | 0,18 | 0,18 |

**Table 3.6 :** Material properties of one layer of UHMWPE [27].

| Elastic modulus (GPa) | | | Density (g/cm$^3$) | | |
|---|---|---|---|---|---|
| $E_z$ | $E_x$ | $E_y$ | | | |
| 153 | 11,3 | 11,3 | 0,97 | | |

| Shear modulus (GPa) | | | Poisson's ratio | | |
|---|---|---|---|---|---|
| $G_{xz}$ | $G_{yz}$ | $G_{xy}$ | $\nu_{xy}$ | $\nu_{yz}$ | $\nu_{xy}$ |
| 6,0 | 6,0 | 3,6 | 0,3 | 0,3 | 0,4 |

| Tensile failure stress Z (GPa) | Tensile failure stress X (GPa) | Compressive failure stress Z (GPa) | Compressive failure stress X (GPa) | Maximum shear stress XZ (GPa) | Maximum shear stress XY (GPa) |
|---|---|---|---|---|---|
| 0,13 | 2,537 | 0,65 | 1,58 | 0,18 | 0,34 |

## 3.2 Effect of Layer Stacking Sequence on Ballistic Response

The previous analysis focused on material effect figured out that the most efficient secondary material besides Kevlar 29/epoxy is UHMWPE. Therefore, 4 different types of layer stacking sequences of these two materials are tested in this subsection. The first one is the layer stacking sequence used in the previous subsection in determining the secondary material, [(K/X)$_9$/K]. The second stacking sequence arrangement is based on sandwich composite systems. It has 5 woven layers of Kevlar 29/epoxy at the top and 5 at the bottom of the plate and 9 woven layers of UHMWPE at the center as core material. The notation is expressed as [K$_5$/U$_9$/K$_5$]. The third stacking sequence is inspired from functionally graded materials (FGMs), where the concentration of one of the component materials decreases as the concentration of the other component material increases in the material depth direction. In the present study, Kevlar 29/epoxy is dominant on the top of the plate while UHMWPE is dominant at the

bottom. The grounds for this arrangement is that the outer slices of the plate are exposed to entire impact energy while the inner slices are exposed to a lower impact energy since part of the energy is absorbed mainly in the outer slices. The stacking sequence of the FGM can be expressed as $[K_5/U_2/K_3/U_3/K_2/U_4]$. The last arrangement is basically a plate with the top part Kevlar 29/epoxy and the bottom part UHMWPE, which has the stacking sequence notation of $[K_{10}/U_9]$. In this case, the projectile encounters 10 layers of Kevlar 29/epoxy first, then it passes through 9 layers of UHMWPE. The initial velocity of the projectile is 500 m/s and the residual velocities after the impact in different layer stacking sequences are shown in Table 3.7.

**Table 3.7 :** Effect of layer stacking sequence on residual velocity of projectile.

| No | Layer stacking sequence of the plate | Residual velocity (m/s) |
|----|--------------------------------------|-------------------------|
| 1 | $[(K/U)_9/K]$ | 300,6 |
| 2 | $[K_5/U_9/K_5]$ | 305,53 |
| 3 | $[K_5/U_2/K_3/U_3/K_2/U_4]$ | 320,40 |
| 4 | $[K_{10}/U_9]$ | 301,68 |

The tests indicated that the first type of sequence, in which each 9 UHMWPE woven layers are placed between two woven layers of Kevlar 29/epoxy, is the most effective one among all of the considered stacking sequences, while the functionally graded inspired sequence is the least effective one.

**3.3 Composite Plate Behavior under Different Impact Velocities**

The essence of this study is to obtain a composite plate lighter and tougher against high velocity impacts than pure Kevlar 29/epoxy plates. In the previous subsections, the most effective materials and stacking sequences were evaluated. To obtain a plate tougher than pure Kevlar 29/epoxy plate, the test plate is modelled with approximately the same weight as the Kevlar 29/epoxy plate with 19 layers. As indicated in Table 3.8, the final test model of this study with 23 layers (152,35 g), is still lighter than the pure Kevlar 29/epoxy model with 19 layers (156,75 g).

**Table 3.8 :** Comparison of 500 m/s impact results of pure Kevlar 29/epoxy and Kevlar 29/epoxy – UHMWPE plates.

| Composition | Total number of layers | Total thickness (mm) | Total weight (g) | Residual velocity of the projectile (m/s) |
|---|---|---|---|---|
| Kevlar 29/epoxy | 19 | 9,5 | 156,75 | 265,49 |
| Kevlar 29/epoxy - UHMWPE | 23 | 11,5 | 152,35 | 241,10 |

Comparison of high velocity (500 m/s) impact results of 19 layers of Kevlar 29/epoxy and 23 layers of Kevlar 29/epoxy – UHMWPE composite indicates that Kevlar 29/epoxy – UHMWPE composite plate decelerates the velocity of the projectile more effectively than Kevlar 29/epoxy plate. The total thickness of the new design is 2 mm greater than the Kevlar 29/epoxy plate, while it is 2,81% lighter in weight.

High velocity ballistic impact response of Kevlar 29/epoxy – UHMWPE composite plate is analysed for different high velocity flat nosed projectile impacts and the results are shown in Table 3.5. For the first three impact velocities, the projectile do not fully penetrate the plate and is recoiled by the plate. For the 300 m/s impact velocity of the projectile, the kinetic energy analysis shows that the plate absorbed almost all of the kinetic energy of the projectile by hardly stopped it; thus, it can be concluded that the ballistic limit of the Kevlar 29/epoxy – UHMWPE plate is about 300 m/s. Above this impact velocity, the projectile passes through the plate. In Table 3.9, the initial and the residual kinetic energies of the projectile are compared. As the impact velocity increases, the rate of energy absorbed by the plate decreases.

**Table 3.9 :** High velocity impact response of Kevlar 29/epoxy – UHMWPE plate with 23 layers to flat nosed Steel 4340 projectile.

| Impact velocity (m/s) | Initial kinetic energy of projectile (j) | Residual velocity of projectile (m/s) | Residual kinetic energy of projectile (j) | Percentage of kinetic energy absorbed by the plate (%) |
|---|---|---|---|---|
| 100 | 30,750 | -37,553 | 4,336 | 100,000 |
| 200 | 123,000 | -33,499 | 3,451 | 100,000 |
| 300 | 276,750 | -0,8334 | 0,002 | 100,000 |
| 400 | 492,000 | 135,390 | 56,366 | 88,543 |
| 500 | 768,750 | 241,100 | 178,747 | 76,748 |
| 600 | 1107,000 | 334,928 | 344,944 | 68,839 |
| 700 | 1506,750 | 447,166 | 614,869 | 59,192 |
| 800 | 1968,000 | 547,878 | 923,024 | 53,098 |
| 900 | 2490,750 | 647,920 | 1290,886 | 48,173 |
| 1000 | 3075,000 | 741,108 | 1688,916 | 45,076 |

Kinetic energy of the projectile is obtained by using kinetic energy formula shown in (3.1).

$$E_k = \frac{1}{2}mv^2 \tag{3.1}$$

The letter $m$ describes mass of the projectile in grams and the letter $v$ describes velocity of the projectile in meters per second. Initial kinetic energy values are calculated with impact velocity values for each scenario in Table 3.5 and an example for calculation of initial kinetic energy of the projectile with an impact velocity of 500 m/s is shown in Equation (3.2). For residual kinetic energy values of the projectile, residual velocity values of the projectile are used and its example is shown in Equation (3.3)

$$E_{k,initial} = \frac{1}{2}(6,15\ g)(500\ m/s)^2 = 768,750\ j \tag{3.2}$$

$$E_{k,residual} = \frac{1}{2}(6,15\ g)(241,1\ m/s)^2 = 178,747\ j \tag{3.3}$$

In Figures 3.1 – 3.2, penetration of the 23 layers of Kevlar 29/epoxy – UHMWPE plate under 500 m/s impact velocity of flat nosed projectile are illustrated. The penetration

result with breakage of the plate zone on the trajectory of the projectile. The whole penetration progress lasts 9,6E-5 s.
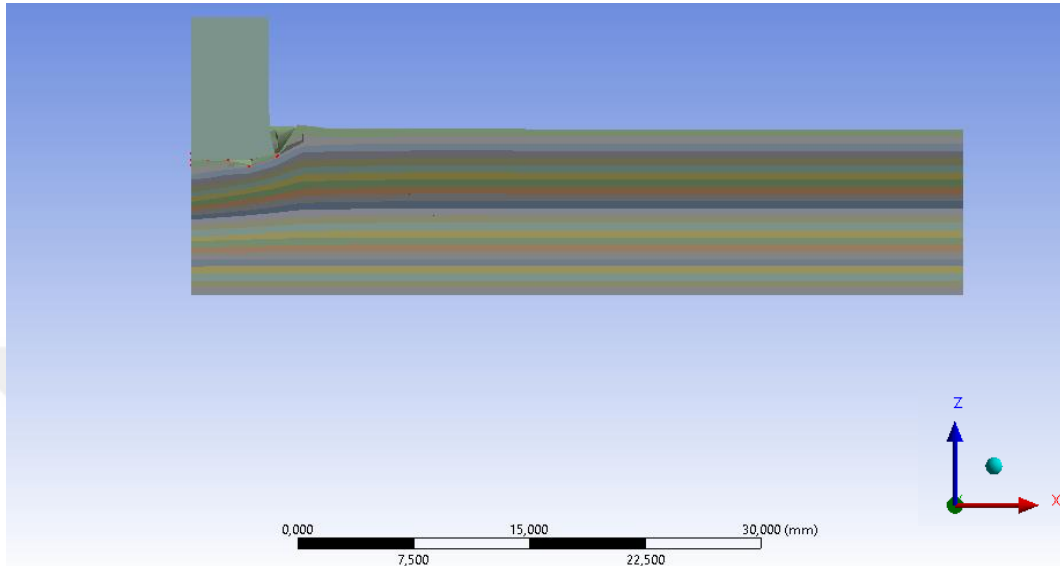


**Figure 3.1 :** Entrance of the projectile at 5,8182E-6 s.
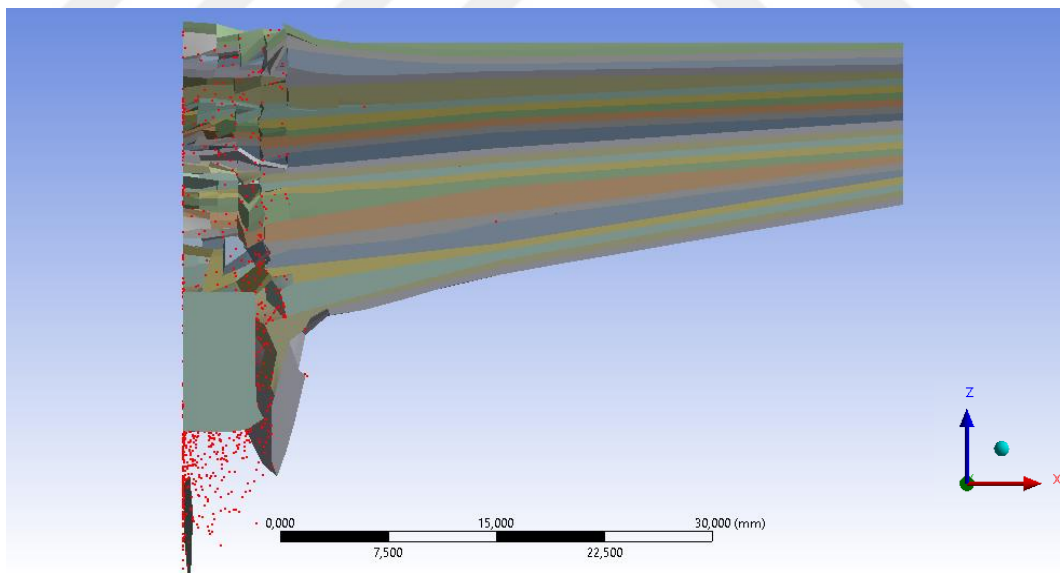


**Figure 3.2 :** Exit of the projectile from the plate at 9,6000E-5 s.

The velocity variations of the projectile during the penetration are plotted for each impact velocity, in Figure 3.3. For the impact velocities that causes perforation,

variation trends are quite similar (top 7 lines in the figure). For the lower impact velocities in which no perforation occurs, the variation trends are not similar to each other because the projectile penetrates different amount of layers for those cases. The negativities of the low velocity trend lines indicates recoil motion of the projectile.
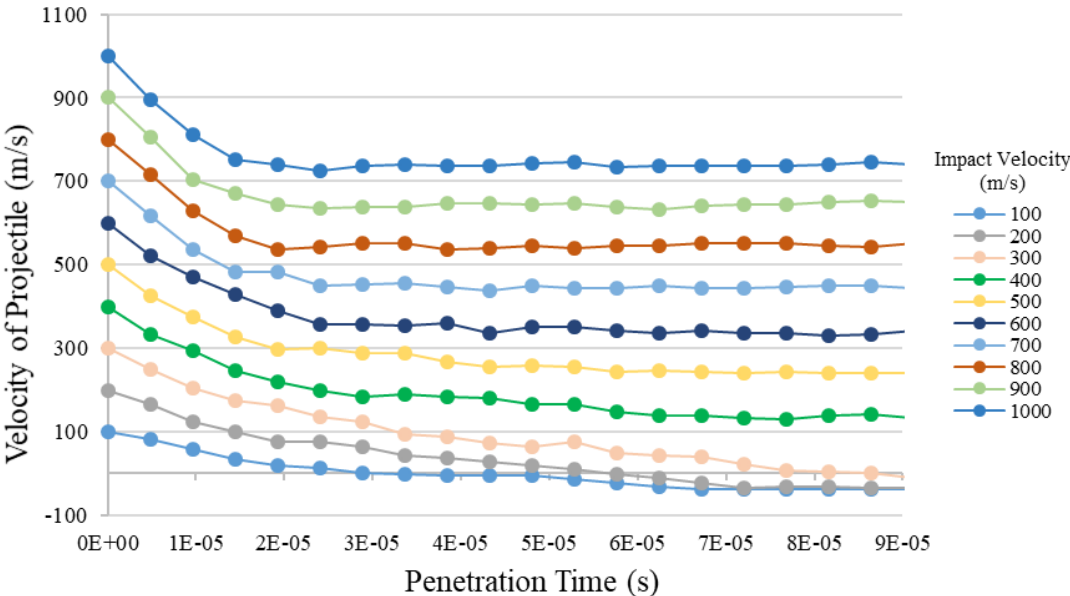


**Figure 3.3 :** Velocity variations of flat nosed projectile during penetration of Kevlar 29/epoxy – UHMWPE for different impact velocities.

The linearity between impact velocities and residual velocities can be seen clearly in Figure 3.4. for perforation cases. The dashed red line is the trend line of the graph line and it almost coincides with the graph line; therefore, the equation of the trend line can also be accepted for the graph line. For partial penetration cases, residual velocity are not measured, thus they are excluded from the graph. For these high-velocities and beyond, the plate decelerates the projectile by the average of 262 m/s based on the trend line equation of the graph.
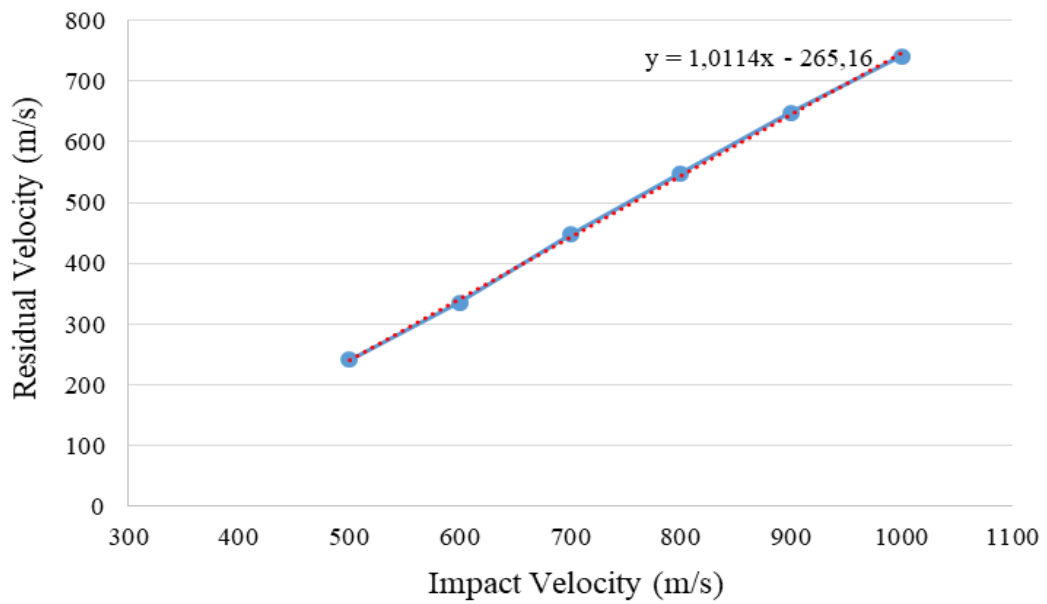
**Figure 3.4 :** Residual velocity variation of flat nosed projectile with impact velocity in Kevlar 29/epoxy – UHMWPE tests.

Variations of kinetic energy of flat nosed Steel 4340 projectile with penetration time are plotted in Figure 3.5. As expected, kinetic energy difference for the residual velocity of the projectile begins after the ballistic limit of the Kevlar 29/epoxy – UHMWPE plate, which is 300 m/s.
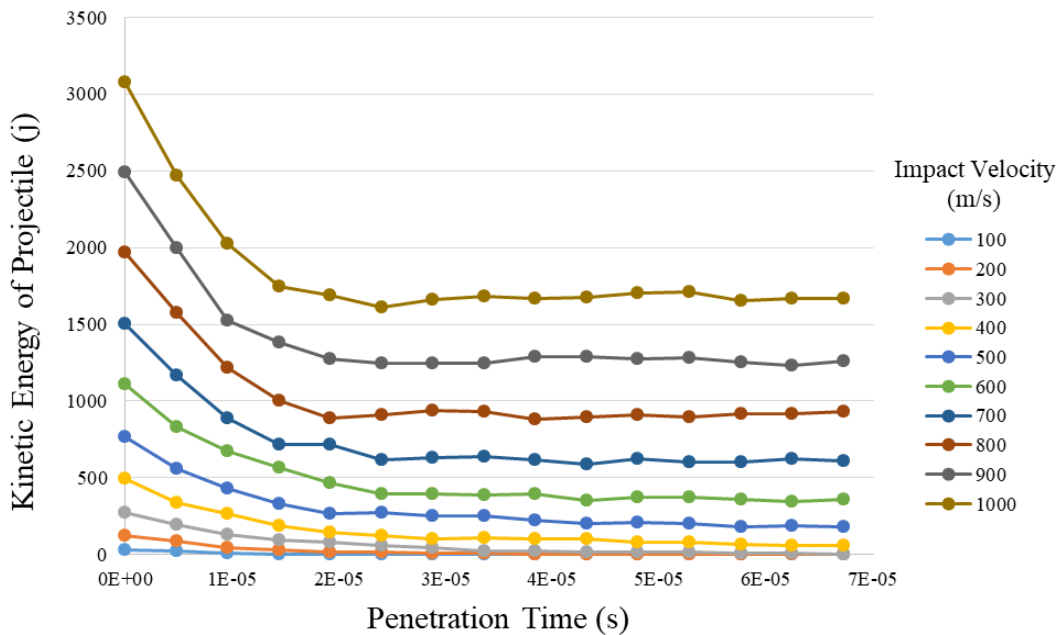
**Figure 3.5 :** Kinetic energy variations of flat nosed projectile with penetration time in Kevlar 29/epoxy – UHMWPE tests.

## 3.4 Effect of Projectile Type on Ballistic Response

In the previous subsection, the flat nosed Steel 4340 projectile has been used for the high velocity impact tests to meet the agreements of the base study. To determine the effect of projectile type, the projectile is modelled with a conical nose, 118° of conical angle. It is expected that the projectile will have greater residual velocity than the flat nosed one for the perforation process. The reason of that expectation is a flat nose pushes more mass of plate material than a conical nose and is exposed to more friction by the plate. The effect of projectile type can be understood by modelling a different shaped projectile with the same weight and with the same material of the flat nosed projectile. The flat nosed Steel 4340 projectile that is used in the previous analyses has a volume of 785,4 mm$^3$ and a mass of 6,15 g. The conical nosed projectile is modelled exactly with the same volume and same mass. In Table 3.10, the residual velocities and absorbed kinetic energies are presented for the high velocity impact of conical nosed Steel 4340 projectile on Kevlar 29/epoxy – UHMWPE plate.

26

**Table 3.10:** High velocity impact response of Kevlar 29/epoxy – UHMWPE plate with 23 layers to conical nosed Steel 4340 projectile.

| Impact velocity (m/s) | Initial kinetic energy of projectile (j) | Residual velocity of projectile (m/s) | Residual kinetic energy of projectile (j) | Percentage of kinetic energy absorbed by the plate (%) |
|---|---|---|---|---|
| 100 | 30,750 | -11,867 | 0,433 | 100,000 |
| 200 | 123,000 | -25,589 | 2,014 | 100,000 |
| 300 | 276,750 | -7,619 | 0,179 | 100,000 |
| 400 | 492,000 | 134,520 | 55,644 | 88,690 |
| 500 | 768,750 | 307,042 | 289,895 | 62,290 |
| 600 | 1107,000 | 404,488 | 503,102 | 54,553 |
| 700 | 1506,750 | 510,690 | 801,973 | 46,775 |
| 800 | 1968,000 | 615,064 | 1163,284 | 40,890 |
| 900 | 2490,750 | 716,052 | 1576,646 | 36,700 |
| 1000 | 3075,000 | 813,422 | 2034,590 | 33,834 |

In Figure 3.6 – 3.7, penetration of the 23 layers of Kevlar 29/epoxy - UHMWPE plate impacted by the conical nosed Steel 4340 projectile is illustrated for 500 m/s impact velocity. The catastrophic failure of the unpenetrated layers occured because of the accumulated tension of potential energy. The penetration resulted with the breakage of the plate zone on the trajectory of the projectile. The whole penetration process lasts 9,6E-5 s.
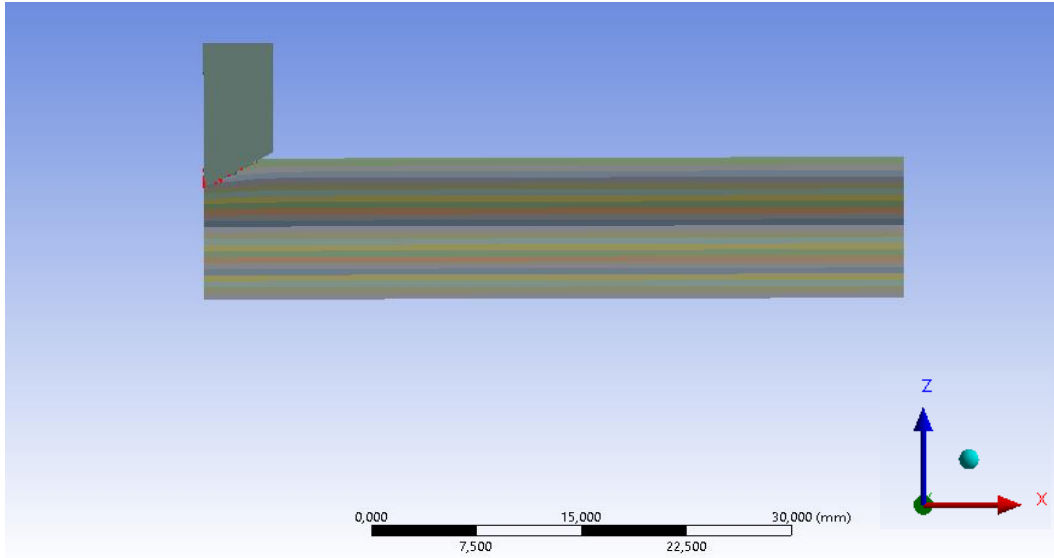
**Figure 3.6 :** Entrance of the projectile at 5,8183E-6 s
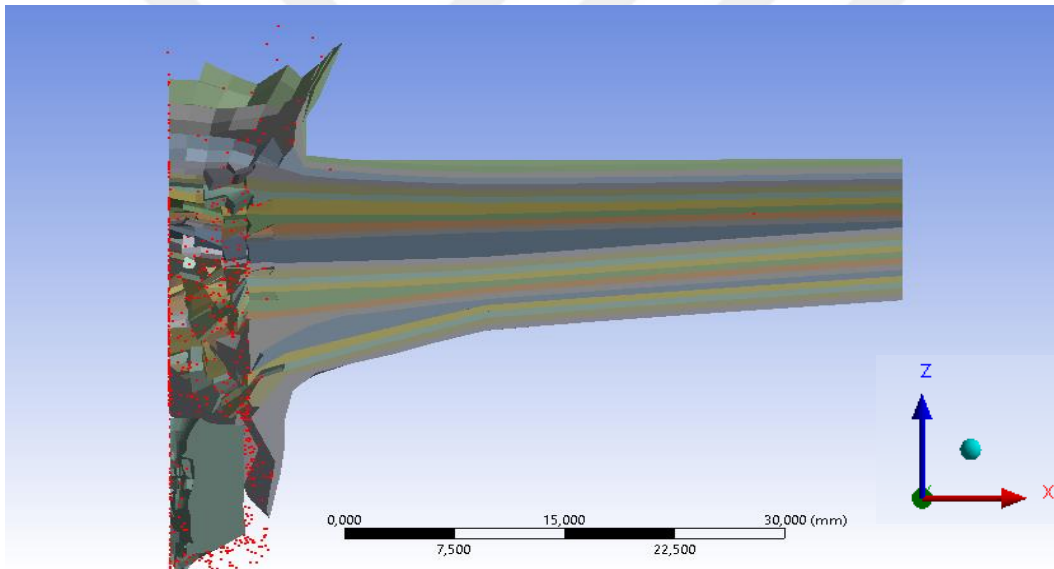


**Figure 3.7 :** Perforation at 9,6000E-5 s.

The biggest difference between the high velocity impact by conical nosed projectile and flat nosed projectile is the form of ejecta on the entrance environment. In any high velocity impact or volcanic eruption, particles that thrown out of a cone or crater are called ejecta. On the surface of the plate impacted by flat nosed projectile, there is a short cone shaped ejecta around the entrance. However, on the surface of the plate impacted by conical nosed projectile there is a cone shaped ejecta with greater height. The reason for the higher formation of the ejecta is the gathering movement of the

28

plate mass on the trajectory. The conical nosed projectile collects the plate part on its trajectory and pushes it out from its center. Then the part of the plate on the trajectory is jammed and erupts from the entrance.

The velocity variations of the projectile during the penetration are plotted for each impact velocity, in Figure 3.8. For the impact velocities that caused full penetration, variation trends are quite similar (top 6 lines in the figure). For the lower impact velocities, in which no perforation occurs, the variation trends are not similar to each other because the projectile penetrates different amount of layers for those cases.
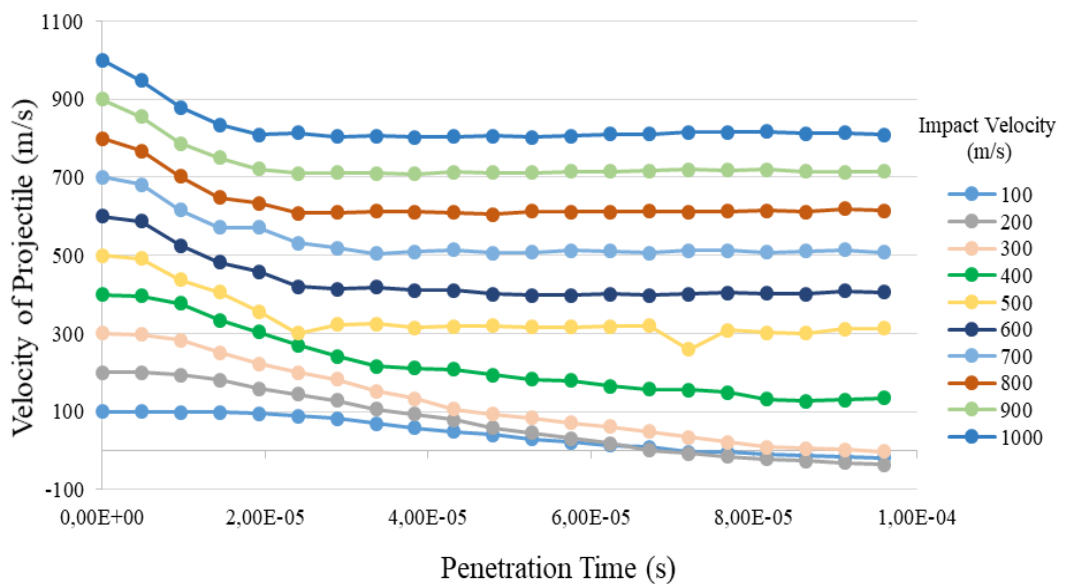


**Figure 3.8 :** Velocity variations of the conical nosed projectile during penetration of Kevlar 29/epoxy – UHMWPE for different impact velocities.

The linearity between impact velocities and residual velocities can be seen clearly in Figure 3.9 for perforation cases. The dashed red line is the trend line of the graph line and it almost coincides with the graph line; therefore, the equation of the trend line can also be accepted for the graph line. For partial penetration cases, residual velocity is not measured, thus excluded from the graph. For these high velocities and beyond, the plate decelerates the projectile by approximately 200 m/s.
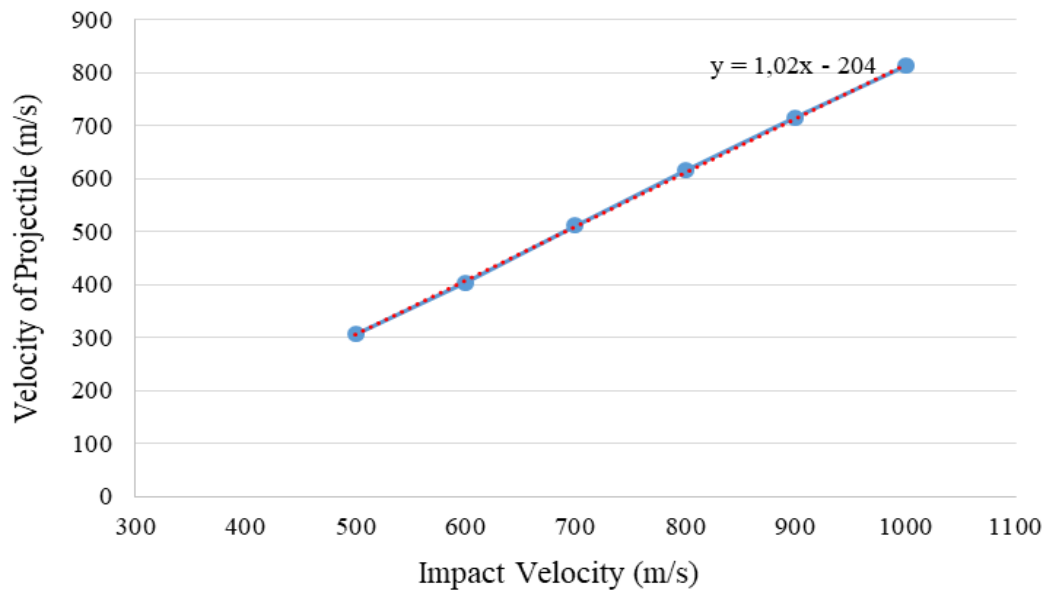
**Figure 3.9 :** Residual velocity variation of conical nosed projectile with impact velocity in Kevlar 29/epoxy – UHMWPE tests.

Variations of kinetic energy of conical nosed projectile with penetration time are plotted in Figure 3.10. As expected, kinetic energy difference for the residual velocity of the projectile began after the ballistic limit of the Kevlar 29/epoxy – UHMWPE plate, which is 300 m/s. It is concluded that the kinetic energy variations of Steel 4340 projectile are proportional to each other for the impact velocities of 500 m/s and above; thus, for any velocity value greater than 500 m/s, kinetic energy variation of the projectile can be obtained depending on Figure 3.10.
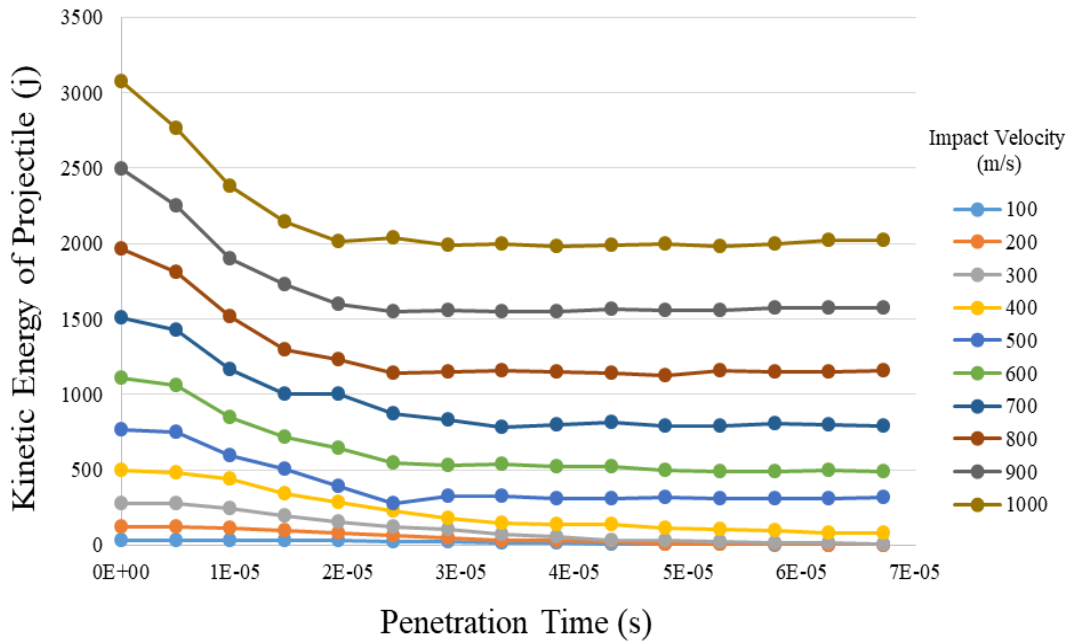
**Figure 3.10 :** Kinetic energy variations of conical nosed projectile with penetration time in Kevlar 29/epoxy – UHMWPE tests.

The velocity variations of projectile during penetration between Kevlar 29/epoxy – UHMWPE plate impacted by flat nosed and conical nosed projectiles are plotted together in Figure 3.11. The graph shows residual velocity variations of two different types of projectiles with penetration time. It is clearly seen that the conical nosed projectile travels faster than the flat nosed projectile, when their impact velocities are the same, which is 500 m/s.



**Figure 3.11 :** Comparison of the velocity variations of conical nosed and flat nosed projectiles during penetration of Kevlar 29/epoxy – UHMWPE plate for impact velocity of 500 m/s.

31

Comparison of residual velocities between conical and flat nosed projectiles is plotted with respect to variation of different impact velocities in Figure 3.12. The comparison indicates that for the impact velocities of higher than 500 m/s, conical nosed projectile leaves Kevlar 29/epoxy – UHMWPE plate with higher velocity than flat nosed projectile.



**Figure 3.12 :** Comparison of the residual velocity variations of conical nosed and flat nosed projectiles during penetration of Kevlar 29/epoxy – UHMWPE plate for different impact velocities.

Kinetic energies of flat nosed and conical nosed projectiles impacted on Kevlar 29/epoxy – UHMWPE plate with the impact velocity of 500 m/s are compared in Figure 3.13. The graphic indicates that kinetic energies of conical nosed projectile are higher than those of flat nosed projectile through the penetration process. The reason is that the instant velocities of conical nosed projectile are higher than those of flat nosed projectile.
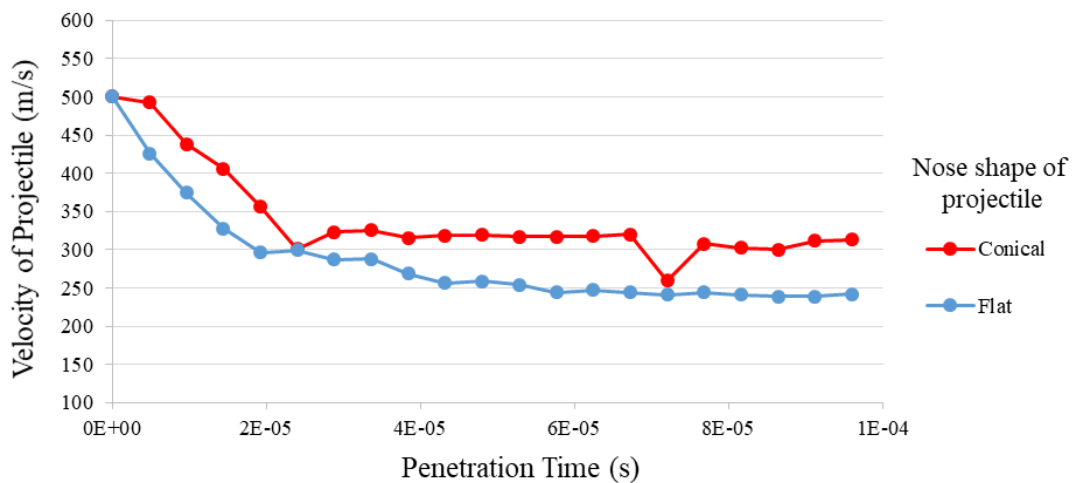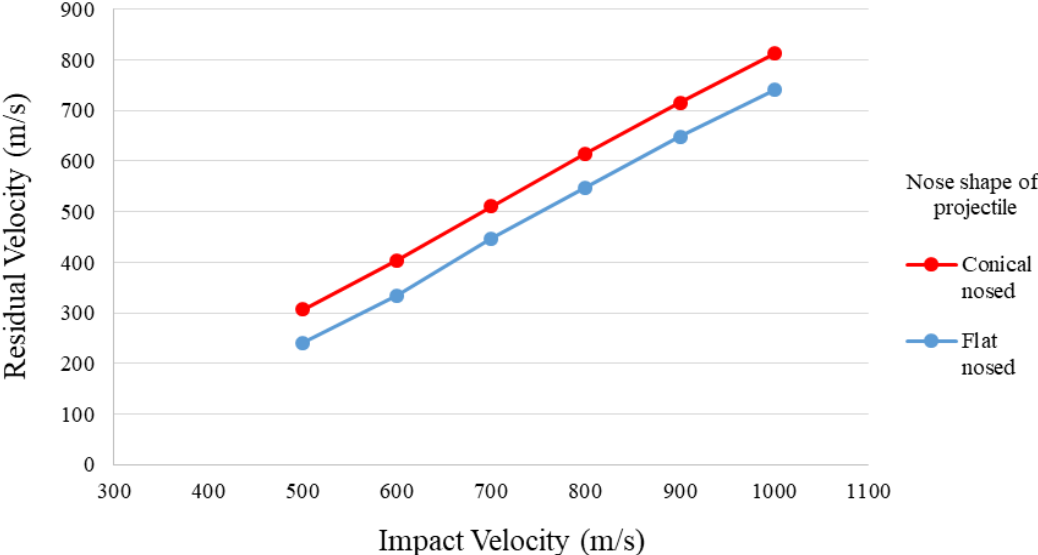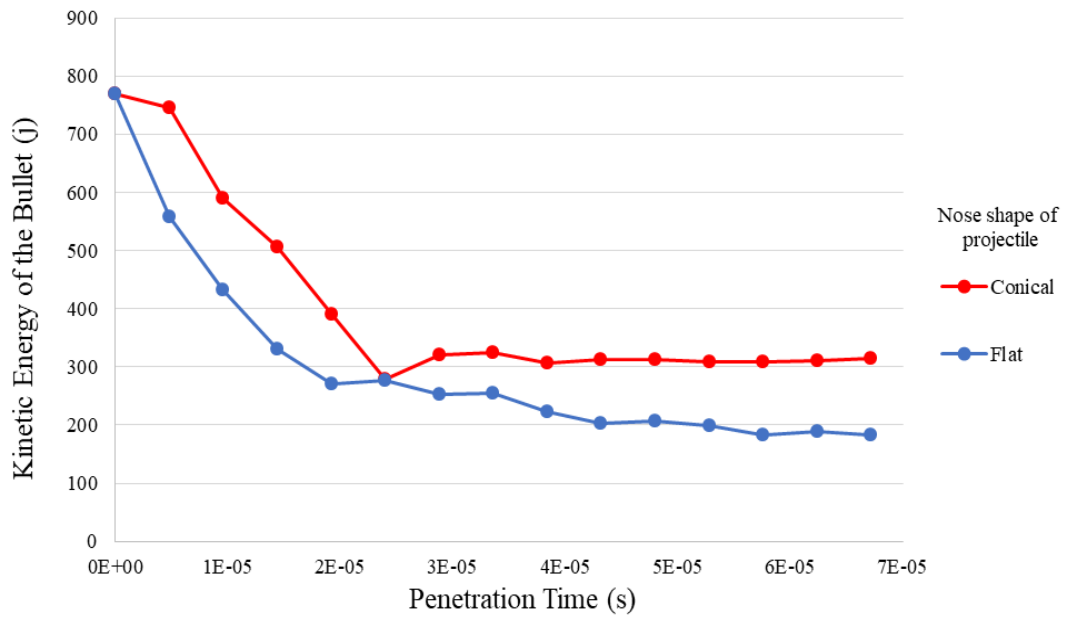
**Figure 3.13 :** Comparison of kinetic energy variations of conical nosed and flat nosed projectiles during penetration of Kevlar 29/epoxy – UHMWPE plate for impact velocity of 500 m/s.

One of the major differences between the high velocity impact responses of Kevlar 29/epoxy – UHMWPE plate impacted by flat nosed and conical nosed projectiles, besides failure propagation pattern, is the percentage of kinetic energy absorbed by the plate. While the projectile mass, plate material, number of layers, velocity of projectile and boundary conditions are the same, kinetic energy absorption of the plate for the two different projectile types are reasonably different due to the shape of the projectile. For the high velocity impact case with flat nosed projectile, the average percentage of kinetic energy absorption of the plate is 62,81%. For the conical nosed projectile, the average percentage of kinetic energy absorption of the plate is 51,96%. According to these results, it is determined that the percentage of kinetic energy absorption of target plate remarkably depends on the shape of projectile.

## 3.5 Effect of Target Plate Shape on Ballistic Response

In this subsection, the effect of target plate shape on high velocity impact response of the plate is studied. In previous tests, rectangular shaped composite plate was tested. In order to determine shape effect of the target plate, a new target plate is modelled with a circular form. Other parameters such as number of layers, layer materials, layer stacking sequence, all clamped boundary conditions, shape of projectile, mesh

convergence and thickness of plate are remained same with the rectangular plate. The circular plate is modelled with a surface area of 100 cm$^2$, the same surface area with the rectangular plate. Radius of the circular plate is 5,64 cm. Velocity of the projectile is defined as 500 m/s and the comparison between results of impact tests of the two plates is done for this impact velocity. Meshing of the laminate is shown in Figure 3.14. In Table 3.11, the residual velocity of the projectile and the kinetic energy absorbed by the plate are presented for the high velocity impact of flat nosed Steel 4340 projectile on circular shaped Kevlar 29/epoxy plate.
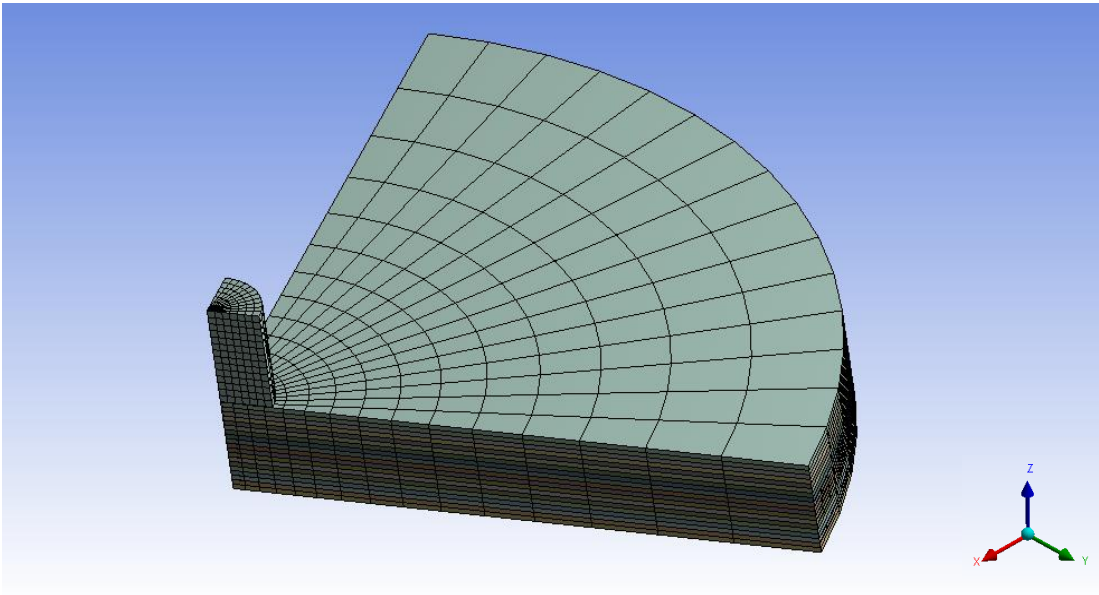


**Figure 3.14 :** Quarter circular plate and flat nosed projectile with 15×15 mesh division.

**Table 3.11 :** High velocity impact response comparison of different shapes of Kevlar 29/epoxy plate with 19 layers to flat nosed Steel 4340 projectile.

| Shape of target plate | Impact velocity (m/s) | Initial kinetic energy of projectile (j) | Residual velocity of projectile (m/s) | Residual kinetic energy of projectile (j) | Percentage of kinetic energy absorbed by the plate (%) |
|---|---|---|---|---|---|
| Circular | 500 | 768,750 | 328,970 | 332,780 | 56,712 |
| Rectangular | 500 | 768,750 | 265,490 | 216,741 | 71,806 |

In Figures 3.15 – 3.16, penetration steps of the 19 layers of Kevlar 29/epoxy circular plate impacted by the flat nosed projectile are visualized. Catastrophic failure of the unpenetrated layers occurs because of the bonding areas that over loaded by kinetic energy between the plies. The next steps are resulted with breakage of the plate zone on the trajectory of the projectile. The whole penetration process lasts 9.6E-5 s.
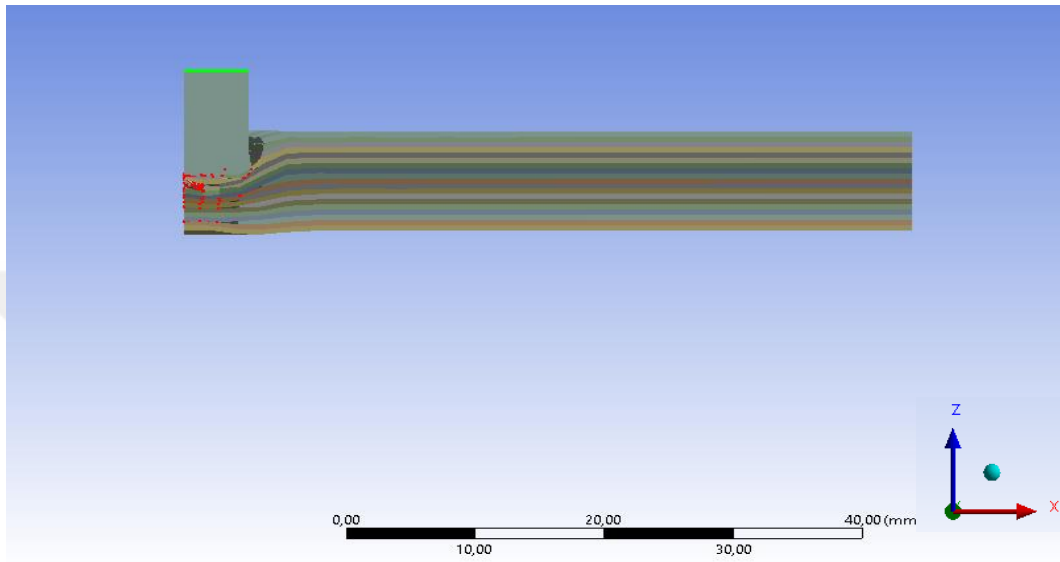


**Figure 3.15 :** Entrance of the projectile at 1,0384E-5 s.

In Figures 3.16 and 3.17, perforation processes of circular and rectangular shaped Kevlar 29/epoxy plates impacted by flat nosed projectile can be seen.
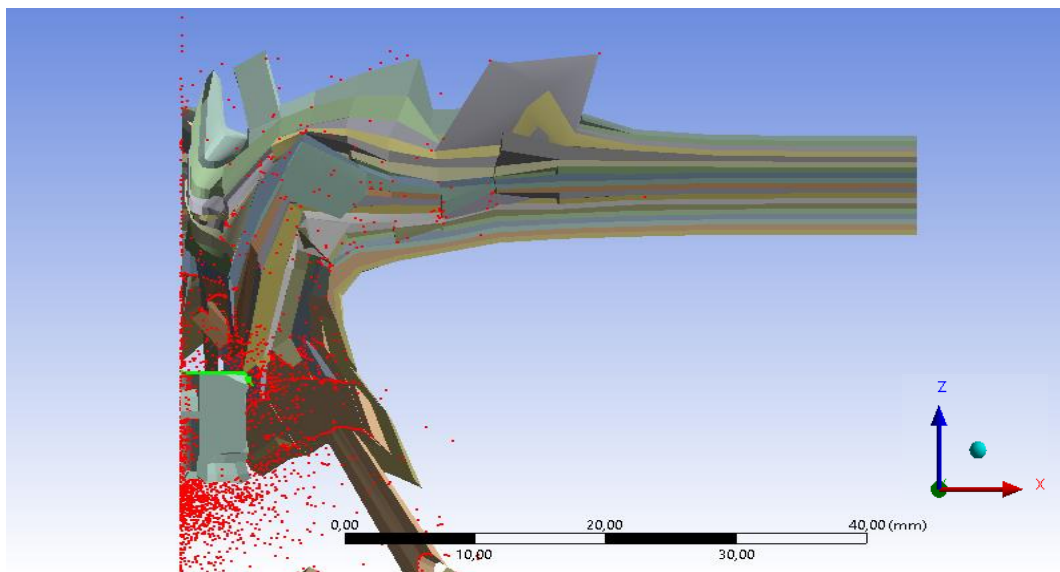


**Figure 3.16:** Post-perforation of circular plate at 9,3460E-5 s.
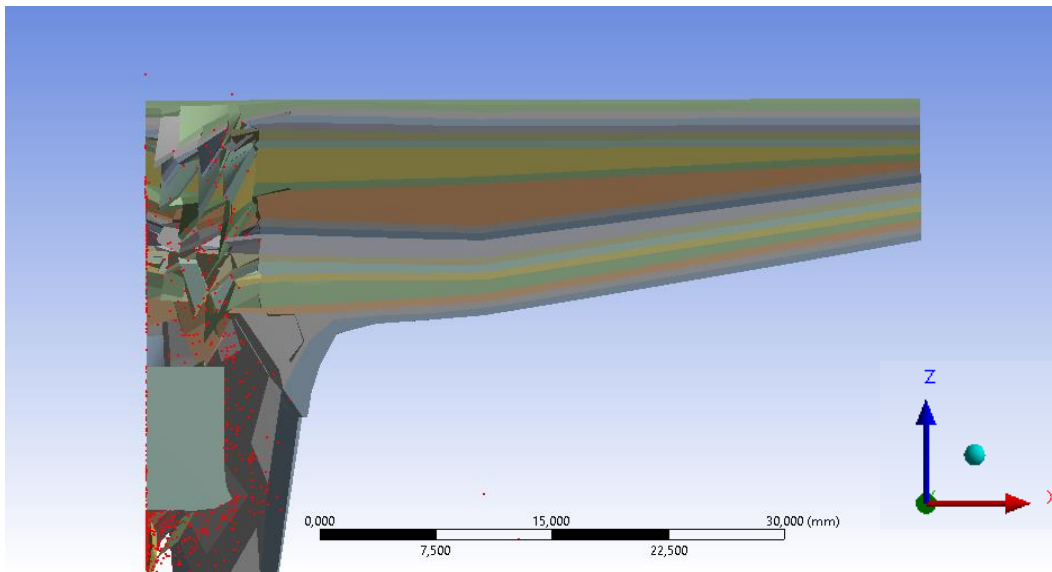
**Figure 3.17 :** Perforation of rectangular Kevlar 29/epoxy plate impacted by flat nosed projectile at 9,6000E-5 s.

The upper part of the circular plate is scattered in a wide area. For the rectangular plate case, there is no any scattering ejecta on the upper plate. The bottom of the two plates also demonstrates different behavior from each other. While the bottom part of the rectangular plate is perforated regularly, the bottom part of the circular plate shows catastrophic scattering.

The velocity variation of projectile during penetration for circular and rectangular shaped Kevlar 29/epoxy plates impacted by flat nosed projectile is plotted as a graph in Figure 3.18. The graph shows residual velocity variations of projectiles impacted on two different types of target plates with penetration time. It is clearly seen that the projectile impacted on circular plate travels faster than the projectile impacted on rectangular plate, whereas their impact velocities are the same, which is 500 m/s.
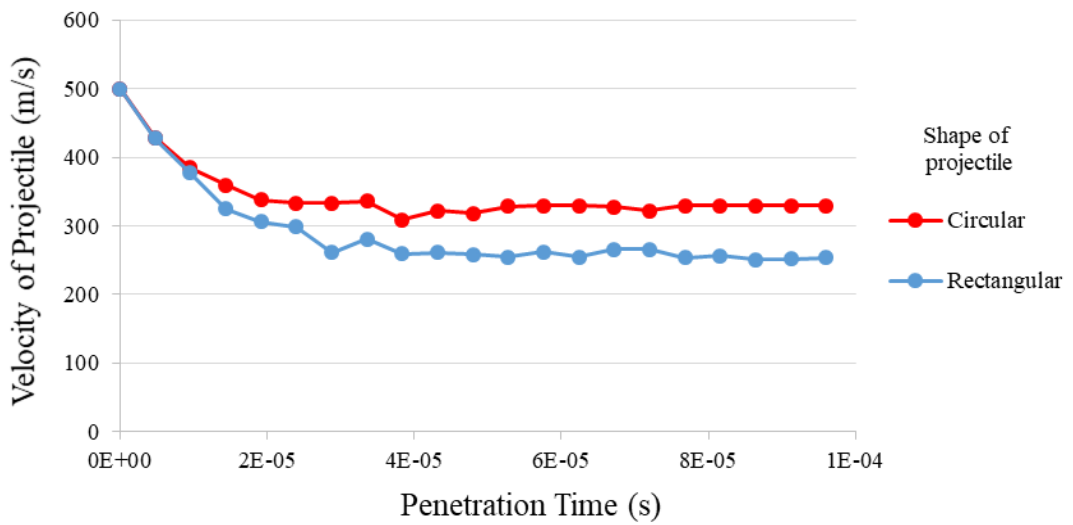
**Figure 3.18 :** Comparison of the velocity variations of flat nosed projectiles during penetration of circular and rectangular Kevlar 29/epoxy plates for impact velocity of 500 m/s.

Kinetic energies of flat nosed projectiles impacted on circular and rectangular shaped Kevlar 29/epoxy target plate with the impact velocity of 500 m/s are compared in Figure 3.19. The graphic indicates that the kinetic energy of flat nosed projectile impacted on circular shaped target plate is higher than the kinetic energy of flat nosed projectile impacted on rectangular shaped target plate through the penetration process.
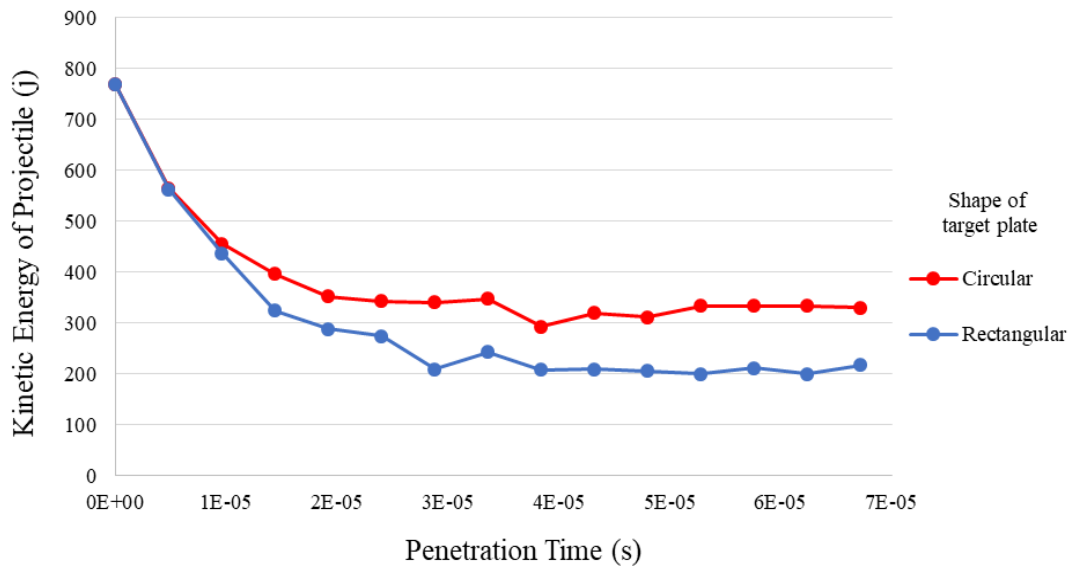
**Figure 3.19 :** Comparison of kinetic energy variations of flat nosed projectiles during penetration of circular and rectangular Kevlar 29/epoxy plates for impact velocity of 500 m/s.

The major differences between the high velocity impact responses of rectangular and circular shaped Kevlar 29/epoxy plates impacted by flat nosed projectile, besides failure propagation pattern, are in the residual velocities of flat nosed projectiles and in the percentage of kinetic energies absorbed by the plate. While the projectile mass, the plate material, the number of layers, the velocity of projectile and the boundary conditions are equal in both plate shapes, kinetic energy absorption of the plates are reasonably different due to their shapes. For the high velocity impact case on rectangular target plate, the average percentage of kinetic energy absorption of the plate is 71,81%, but for the circular target plate, this value is 56,71%. According to these results, it is determined that the percentage of kinetic energy absorption of target plate remarkably depends on its shape.

## 3.6 Impact Tests with a Standard Projectile Model

In order to obtain the response of Kevlar 29/epoxy - UHMWPE plate subjected to real life impact parameters, a standard shaped projectile is tested besides flat nosed and conical nosed projectiles. 9 mm of nominal bullet diameter and full metal jacket (FMJ) projectile is selected for the standard shaped projectile tests to approximate real life standards. The 9 mm elliptical FMJ projectile is modelled according to the dimensions

described in American National Standards Institute and Sporting Arms and Ammunition Manufacturers Institute (ANSI/SAAMI Z299.3 – 2015) standards [28]. As shown in Figure 3.20, the projectile is modelled with a copper jacket and a lead core and the weight of the 9 mm FMJ projectile is 8 grams (Table 3.12). The impact velocity is defined equal to the standard muzzle velocity of 9 mm FMJ projectile, which is 381 m/s. In Table 3.13, the residual velocity of the projectile and recoiled kinetic energy by the plate are presented for the high velocity impact of 9 mm FMJ projectile on Kevlar 29/epoxy – UHMWPE target plate. Recoil energy defines residual kinetic energy of projectile.
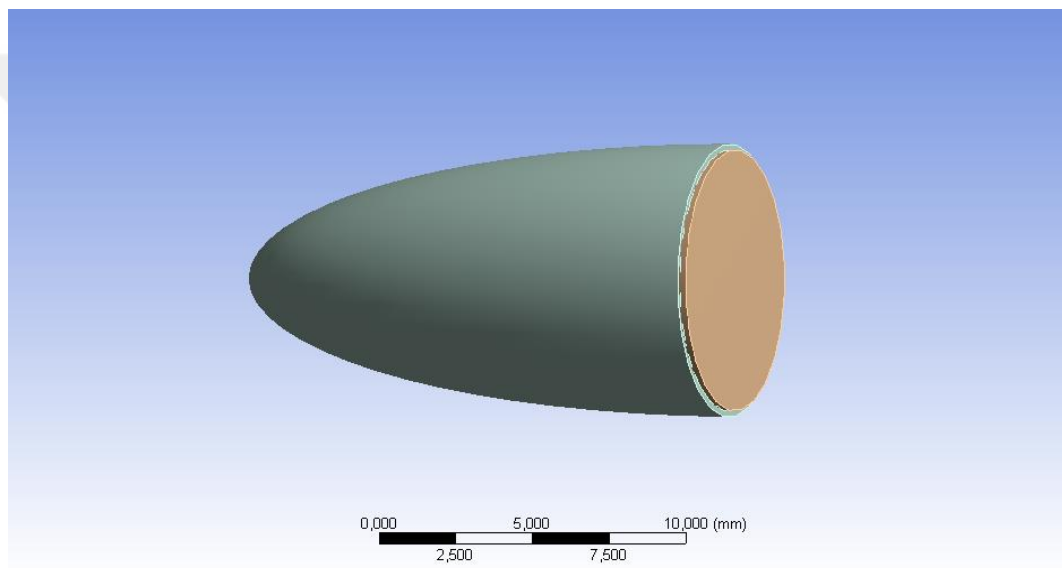


**Figure 3.20 :** The 9 mm FMJ projectile model with lead core and copper jacket.

**Table 3.12 :** Material properties of Lead and Copper.

| Material | Density (kg/m$^3$) | Shear modulus (GPa) | Specific heat (J/kgC°) |
|---|---|---|---|
| Lead | 11340 | 8,6 | 124 |
| Copper | 8900 | 46,4 | 1E-12 |

**Table 3.13 :** High velocity impact response of Kevlar 29/epoxy – UHMWPE plate with 23 layers to 9 mm FMJ projectile.

| Impact velocity (m/s) | Initial kinetic energy of projectile (j) | Residual velocity of projectile (m/s) | Recoil energy of projectile (j) | Percentage of kinetic energy recoiled by the plate (%) |
|---|---|---|---|---|
| 381 | 580,644 | -57,534 | 13,241 | 2,280 |

39

In Figures 3.21 – 3.22, penetration steps of the 23 layers of Kevlar 29/epoxy - UHMWPE rectangular plate impacted by the standard bullet model of 9 mm FMJ projectile are visualized. There is not any catastrophic failure of the layers because the projectile could not perforate the plate, only gets through until one third of the plate thickness. The projectile is flattened under the pressure of its kinetic energy and the reaction of the plate. The whole penetration process lasted 1E-4 s. The reason for the failure of the 9 mm FMJ projectile to perforate the plate is its lower initial kinetic energy than the initial kinetic energy of Steel 4340 projectile mentioned in previous sections.
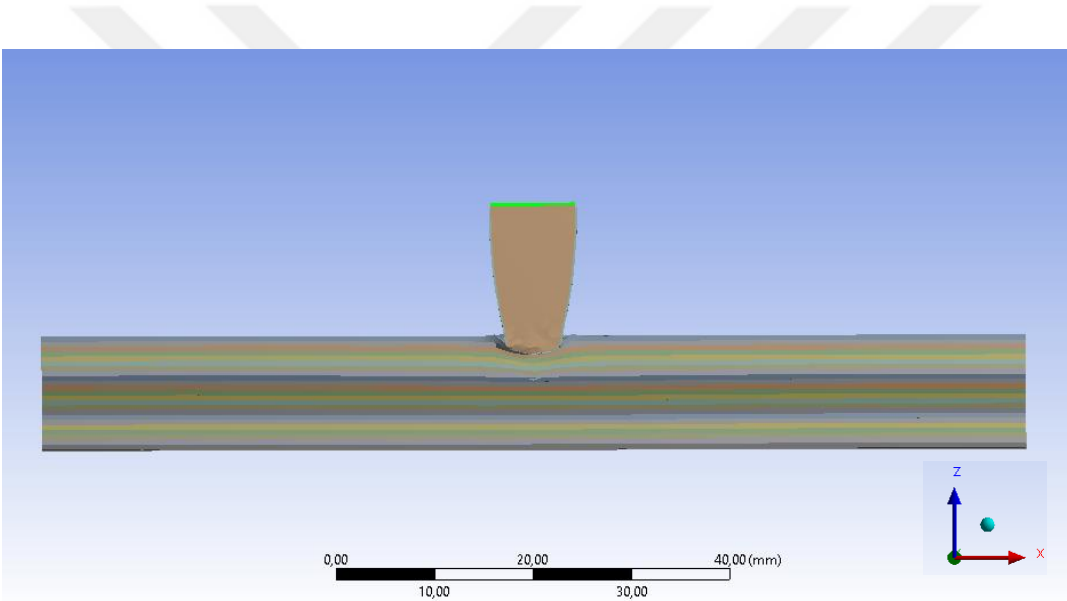


**Figure 3.21 :** Entrance of the projectile at 1.1111E-5 s.
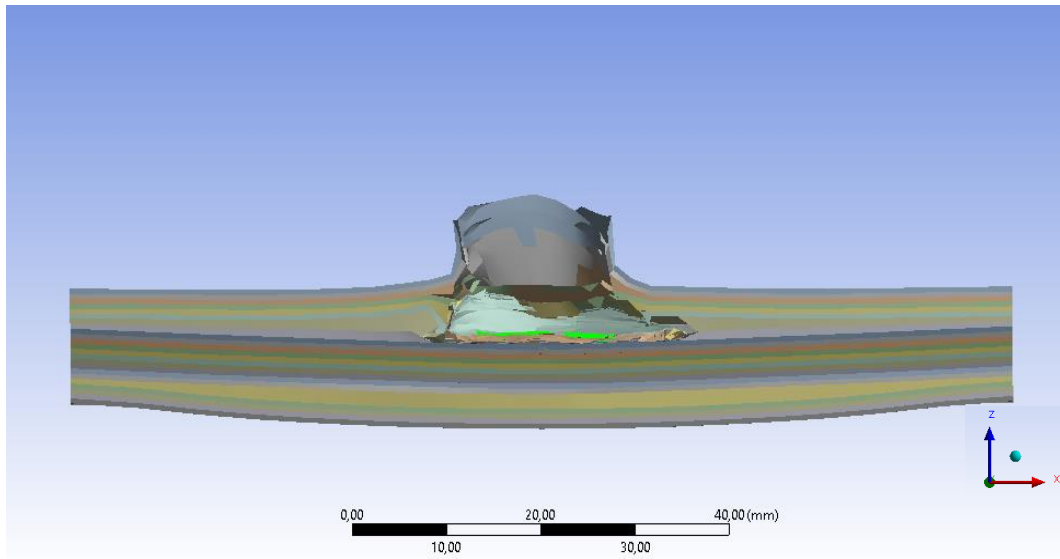
**Figure 3.22 :** Fully flattened projectile with highest cone at 1E-4 s, recoiling of the plate.

The velocity variation of projectile during penetration of rectangular shaped Kevlar 29/epoxy - UHMWPE plate impacted by 9mm FMJ projectile is plotted in Figure 3.23. The graph shows residual velocity variation of the projectile impacted on the target plate with penetration time. Negative velocity values indicate that the projectile is recoiled by the plate at the end of the impact process. The impact velocity of the projectile is defined as 381 m/s, which is the standard velocity for 9 mm FMJ bullet [28].
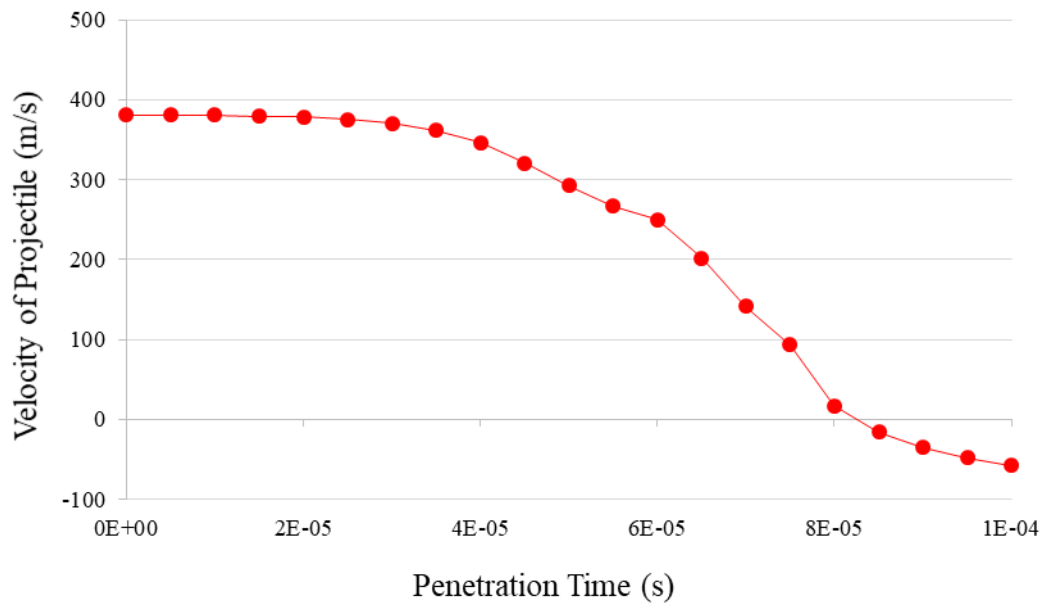
**Figure 3.23 :** Velocity variation of 9 mm FMJ projectile during penetration of rectangular Kevlar 29/epoxy - UHMWPE plate for impact velocity of 381 m/s.

Kinetic energy variation of 9 mm FMJ projectile impacted on rectangular shaped Kevlar 29/epoxy - UHMWPE target plate with the impact velocity of 500 m/s is plotted in Figure 3.24. The rising end of the graph line indicates that the projectile is repelled by the plate and gained velocity in the opposite direction of the impact direction.
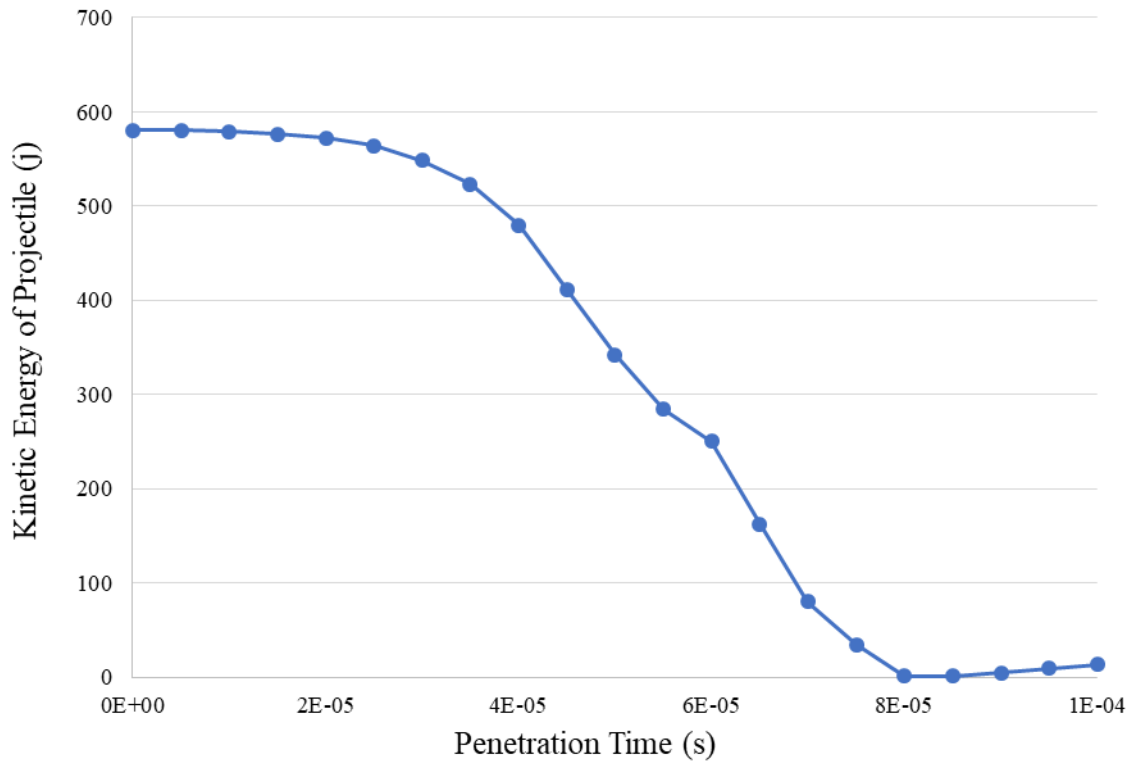
**Figure 3.24 :** Kinetic energy variation of 9 mm FMJ projectile during penetration of rectangular Kevlar 29/epoxy - UHMWPE plate for impact velocity of 381 m/s.

The investigation of high velocity impact with a standard bullet model shows that 23 layers of Kevlar 29/epoxy – UHMWPE plate can easily stop a 9 mm FMJ bullet with an impact velocity of 381 m/s. It is also seen that 6,15 g. Steel 4340 projectile is more effective at penetrating a target plate when impacted with high velocity than 9 mm FMJ bullet with a mass of 8 g. Because of of that, it is safer to use Steel 4340 projectile than 9 mm FMJ bullet model when testing target plates.

## 3.7 Effect of Impact Obliquity of Projectile on Ballistic Response

In real life, perfectly vertical impacts hardly occur. When two or more objects are collided, the angle between the colliders is usually different than 90°. Depending on material properties, shapes and impact velocities of the colliders; obliquity of the impact can result in many different scenarios. In order to obtain the effect of impact obliquity, a FE model has been made with the same conditions of the model in the previous subsection. The standard bullet model of 9 mm FMJ projectile is impacted with its standard impact velocity on a rectangular shaped Kevlar 29/epoxy –

UHMWPE composite target plate with three different impact angles and the results are compared for residual velocities in impact test for vertical direction and kinetic energies of projectiles in Table 3.14. The reason of using only vertical components of projectile velocity to the lateral surface of target plate (z-axis) is to obtain exact residual velocity results relative to the bottom surface of the plate during impact process. If total velocity values were used, the x and y axis components of velocity would not be considered independently and the velocity of projectile could not be obtained along the depth of target plate. These values are still comparable since the total velocity of the projectile is the same, 381 m/s. Obliquity values are in degrees and they represent the angles between the projectile direction and the surface plane of the plate (Figure 3.25).
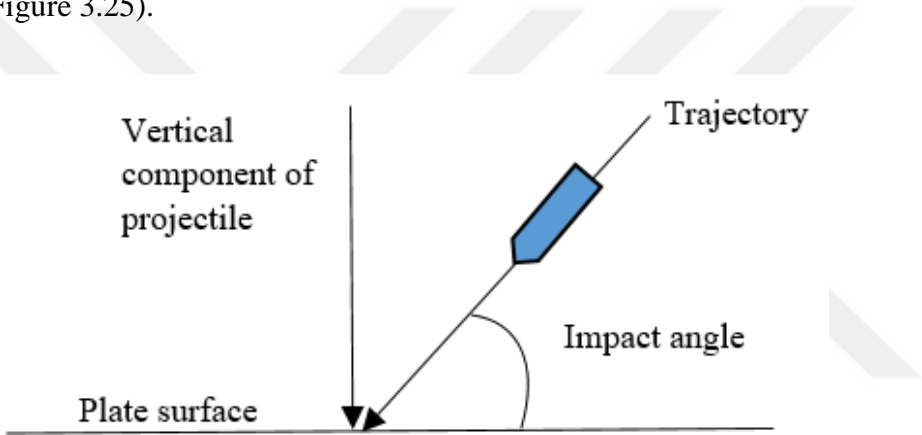


**Figure 3.25 :** Illustration of projectile impact angle.

**Table 3.14 :** High velocity oblique impact response comparison of Kevlar 29/epoxy – UHMWPE plate with 23 layers to 9 mm FMJ projectile.

| Impact angle (°) | Vertical component of impact velocity of projectile (m/s) | Initial kinetic energy of projectile (j) | Vertical component of residual velocity of projectile (m/s) | Recoil energy of projectile (j) | Percentage of kinetic energy recoiled by the plate (%) |
|---|---|---|---|---|---|
| 45 | 269,410 | 580,644 | -6,550 | 191,108 | 32,913 |
| 60 | 329,960 | 580,644 | -22,349 | 76,485 | 13,172 |
| 75 | 368,020 | 580,644 | -116,980 | 94,876 | 16,340 |
| 90 | 381,000 | 580,644 | -57,534 | 13,241 | 2,280 |

In Figures 3.26 – 3.27, penetration steps of the 23 layers of Kevlar 29/epoxy - UHMWPE rectangular plate impacted by the standard bullet model of 9 mm FMJ projectile with 75° impact angle are visualized. When the projectile reaches one third of the plate thickness, initial cone rising can be spotted at the entrance zone. The entrance cone rises towards the opposite direction of obliquity of the projectile. The projectile only gets through until almost half of the plate thickness, 10/23 layers in exact terms. The projectile is flattened under the pressure of its kinetic energy and the reaction of the plate. The whole penetration process lasts 1E-4 s.



**Figure 3.26 :** Entrance of the projectile at 1,1111E-5 s.
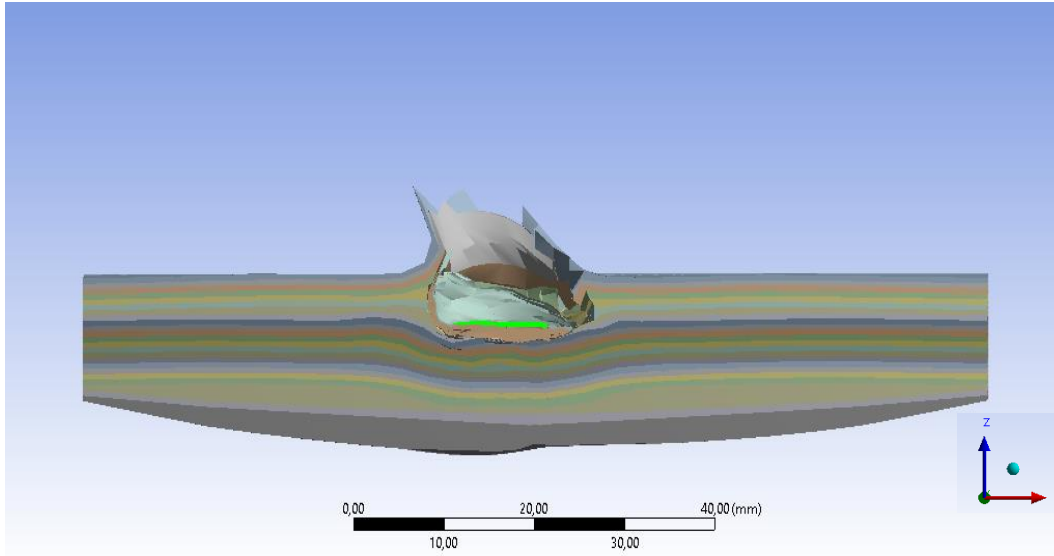
**Figure 3.27 :** Fully flattened projectile with highest cone at 1E-4 s, recoiling of the plate.

In Figures 3.28 – 3.29, penetration steps of the 23 layers of Kevlar 29/epoxy - UHMWPE rectangular plate impacted by the standard bullet model of 9 mm FMJ projectile with 60° impact angle are visualized. When the projectile reaches quarter of the plate thickness, initial cone rising can be spotted at the entrance zone. From the beginning of the formation, the entrance cone rises towards the opposite direction of obliquity of the projectile. The projectile only gets through until one third of the plate thickness. The projectile is flattened under the pressure of its kinetic energy and the reaction of the plate. The whole penetration process lasts 1E-4 s.
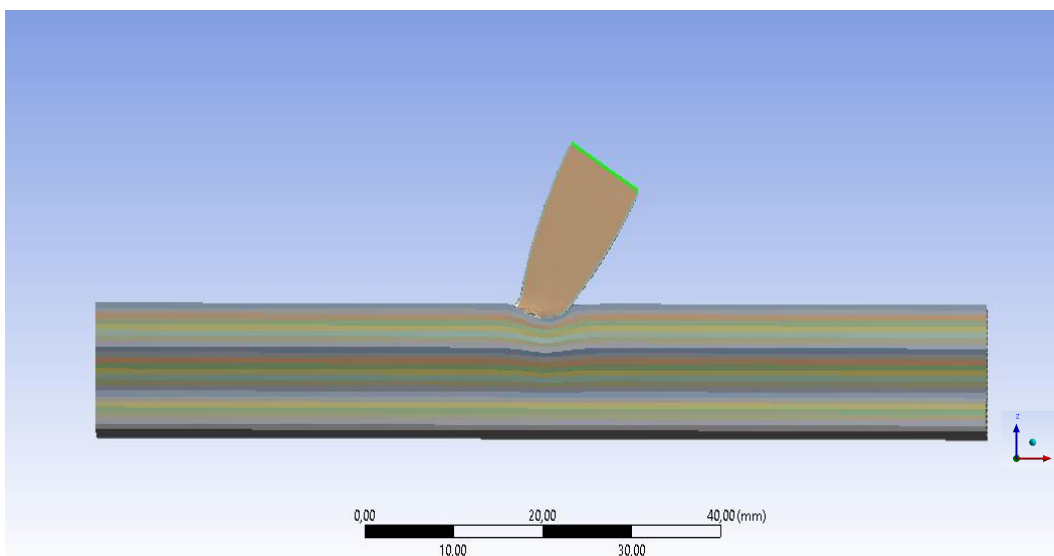


**Figure 3.28 :** Entrance of the projectile at 1,1111E-5 s.
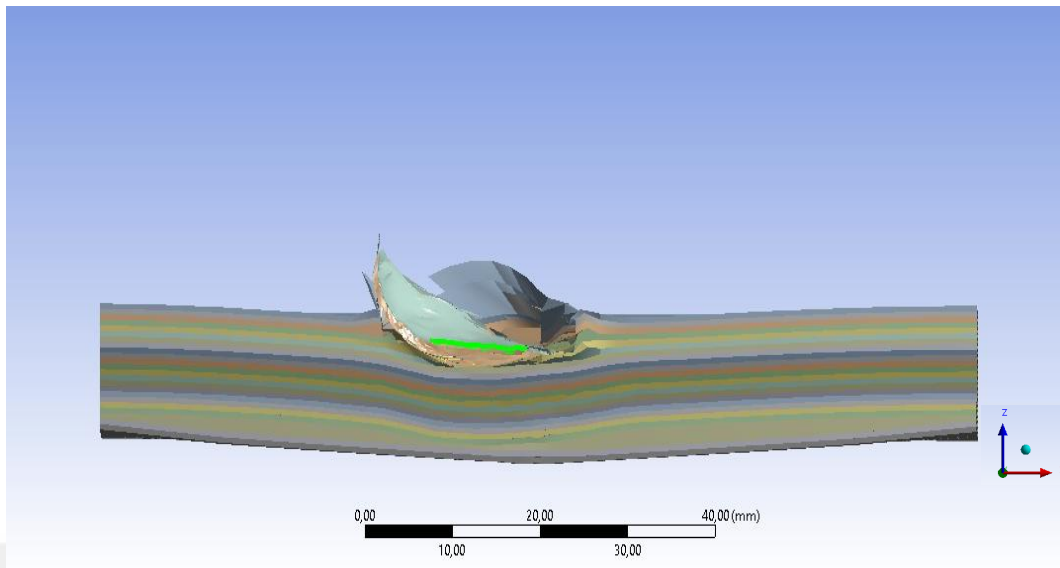
**Figure 3.29 :** Fully flattened projectile with highest cone at 1E-4 s, recoiling of the plate.

In Figures 3.30 – 3.31, penetration steps of the 23 layers of Kevlar 29/epoxy - UHMWPE rectangular plate impacted by the standard bullet model of 9 mm FMJ projectile with 45° impact angle are visualized. When the projectile reaches one sixth of the plate thickness, initial cone rising can be spotted at the entrance zone. From the beginning of the formation, the entrance cone rises towards the opposite direction of obliquity of the projectile. A fluctuation movement is observed at the bottom of the Kevlar 29/epoxy – UHMWPE composite plate (Figure 3.31). The projectile only gets through until one fifth of the plate thickness. The projectile is flattened under the pressure of its kinetic energy and the reaction of the plate. The whole penetration process lasts 1E-4 s.
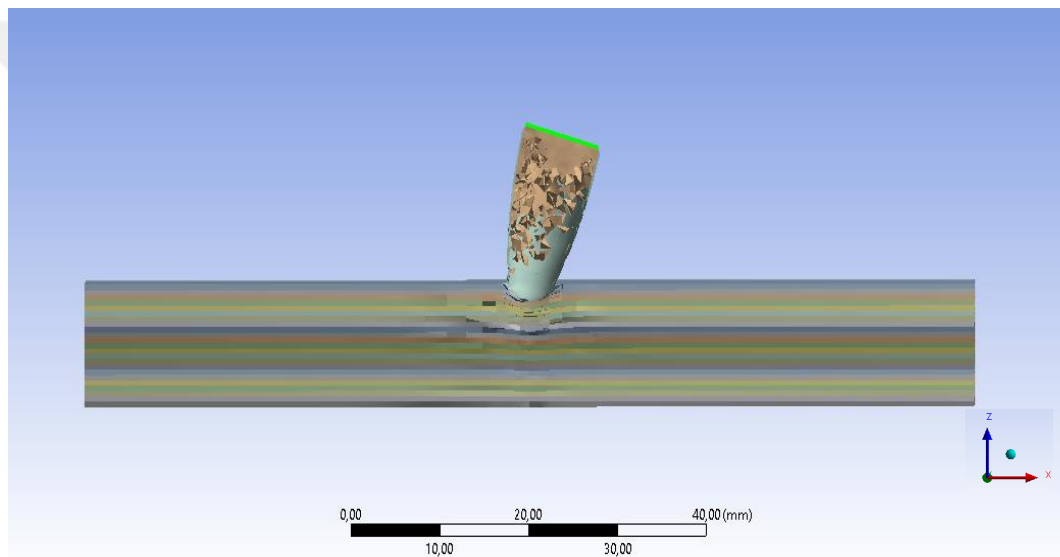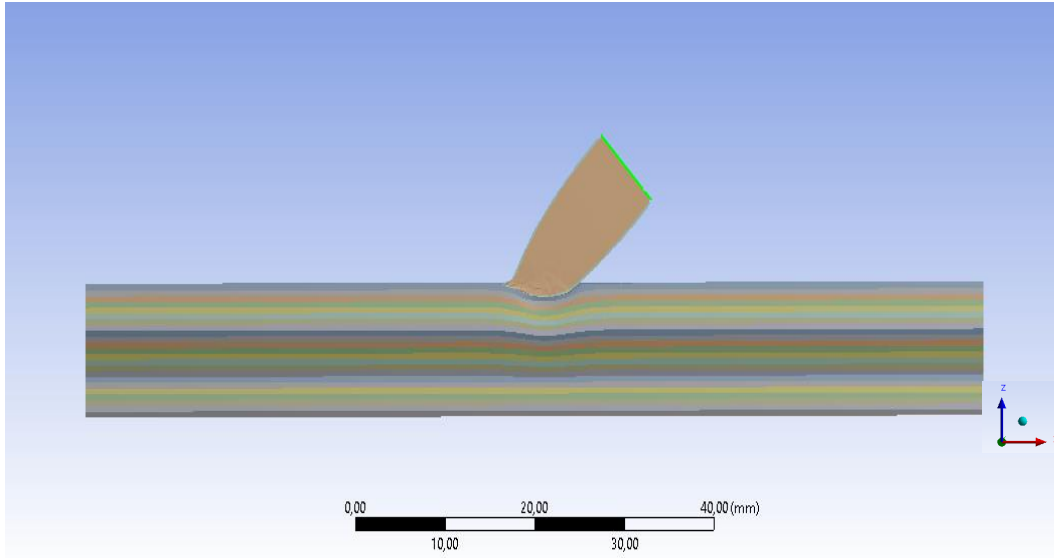
**Figure 3.30 :** Entrance of the projectile at 1,1111E-5 s.
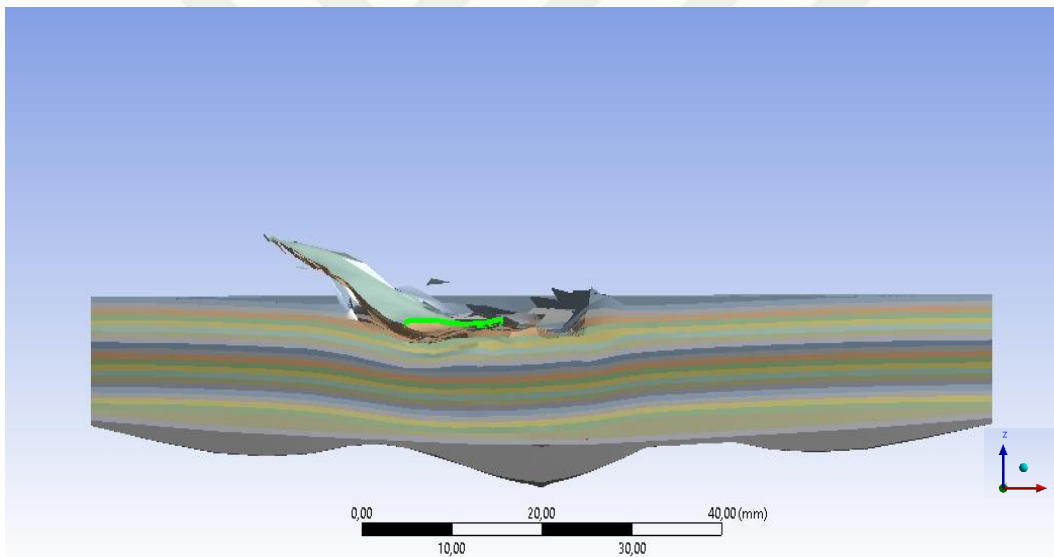


**Figure 3.31 :** Fully flattened projectile with highest cone at 1E-4 s, recoiling of the plate.

Comparison of the velocity component variations in vertical direction and kinetic energy variations of 9 mm FMJ projectiles during penetration of rectangular Kevlar 29/epoxy - UHMWPE plates for different impact angles are plotted in Figure 3.32 and Figure 3.33. In these graphs, the effects of impact angles are compared for 45°, 60°, 75° and 90°.
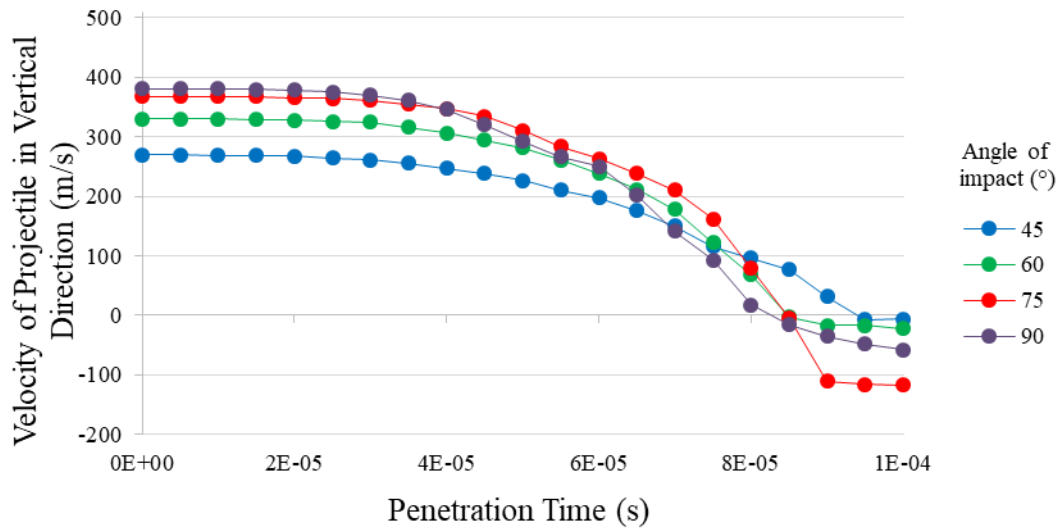
**Figure 3.32 :** Comparison of the velocity component variations in vertical direction of 9 mm FMJ projectiles during penetration of rectangular Kevlar 29/epoxy - UHMWPE plates for different impact angles.
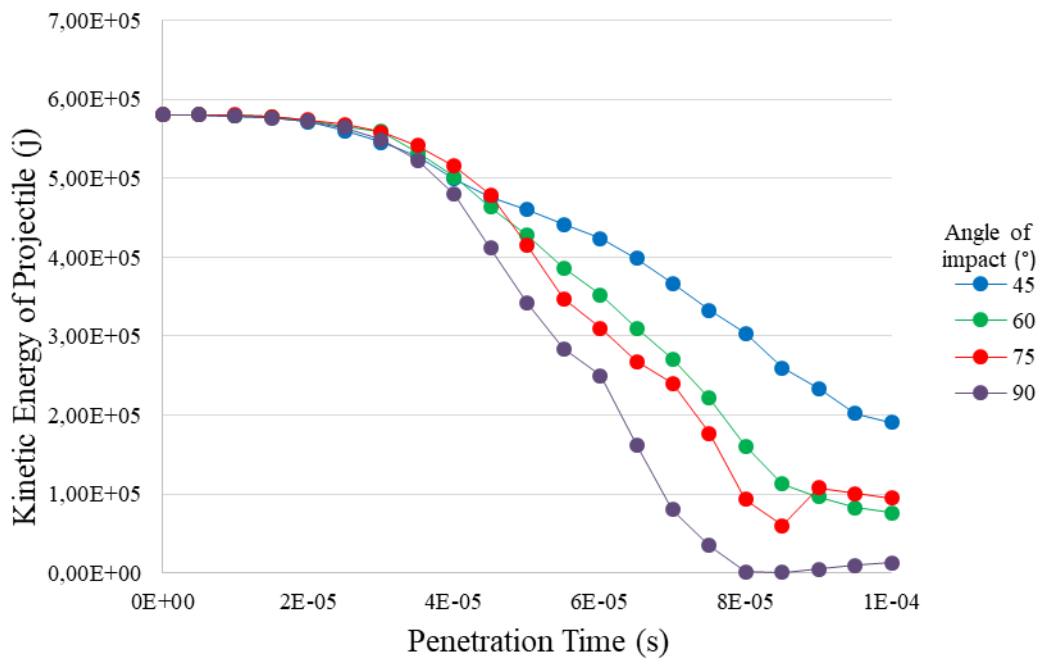


**Figure 3.33 :** Comparison of kinetic energy variations of 9 mm FMJ projectiles during penetration of rectangular Kevlar 29/epoxy - UHMWPE plates for different impact angles.

One of the major differences between the high velocity oblique impact responses of Kevlar 29/epoxy – UHMWPE plates impacted by 9 mm FMJ projectiles is the percentage of kinetic energy recoiled by the plate. While the projectile mass, the plate

material, the number of layers, the velocity of projectile and the boundary conditions are equal, recoil energy of the plate for the four different scenarios are reasonably different due to impact obliquity. As mentioned in Table 3.9, for the impact angle of 45°, the percentage of kinetic energy recoiled by the plate is 32,913%; for the impact angle of 60°, the percentage of kinetic energy recoiled by the plate is 13,172%; for the impact angle of 75°, the percentage of kinetic energy recoiled by the plate is 16,340% and for the impact angle of 90°, the percentage of kinetic energy recoiled by the plate is 2,280%. According to these results, it is obvious that the percentage of kinetic energy recoiled by the target plate depends substantially on the angle of impact. Despite the uncertainty between the results for 60° and 75° impacts, it can be said that percentage of kinetic energy recoiled by the plate increases while impact angle between projectile and target plate decreases. For the impact with 45° obliquity, a fluctuation movement is observed during the penetration process. The reason of this movement is conduction and interference of absorbed kinetic energy of projectile between the layers.

## 3.8 Central Deflection of Plate for Different High Velocity Impact Cases

One of the important parameters for ballistic tests is central deflection of the plate. The importance of this parameter is about protecting the asset not just from projectile impacts, but also from any potential damage that can occur by the central deflection of ballistic plate. Even if the projectile can not perforate the ballistic plate, the central deflection of the plate can cause harm on the protected asset. Because of this hazard, central deflection of the bottom part of a ballistic plate must be investigated.

In the present study, 3 different cases are investigated about central deflection of the plates and the results are presented in Table 3.15. By performing these studies, the effects of plate component materials, projectile shape and target plate shape are concluded.

**Table 3.15 :** Comparison of central deflections for different impact scenarios.

| 300 m/s impact scenario | Central deflection of bottom part of the plate (mm) |
|---|---|
| 19 layers of Kevlar 29/epoxy rectangular plate impacted by flat nosed projectile | 5,6402 |
| 23 layers of Kevlar 29/epoxy – UHMWPE rectangular plate impacted by flat nosed projectile | 4,6491 |
| 23 layers of Kevlar 29/epoxy – UHMWPE rectangular plate impacted by conical nosed projectile | 6,2929 |

According to the results, 19 layers of Kevlar 29/epoxy plate deflects more than 23 layers of Kevlar 29/epoxy – UHMWPE plate under 300 m/s projectile impact. This plate with UHMWPE was mentioned before as lighter and better at decelerating projectile than 19 layers of Kevlar 29/epoxy plate and it also deflects less than its heavier competitor. These results proves that 23 layers of Kevlar 29/epoxy – UHMWPE plate is better than 19 layers of Kevlar 29/epoxy plate in every ballistic terms.

In Figure 3.34, central deflection of the bottom layer of 23 layered Kevlar 29/epoxy – UHMWPE rectangular plate impacted by 300 m/s velocity of flat nosed Steel 4340 projectile is illustrated. The graph line shows exact motion of the point with a fluctuation movement.
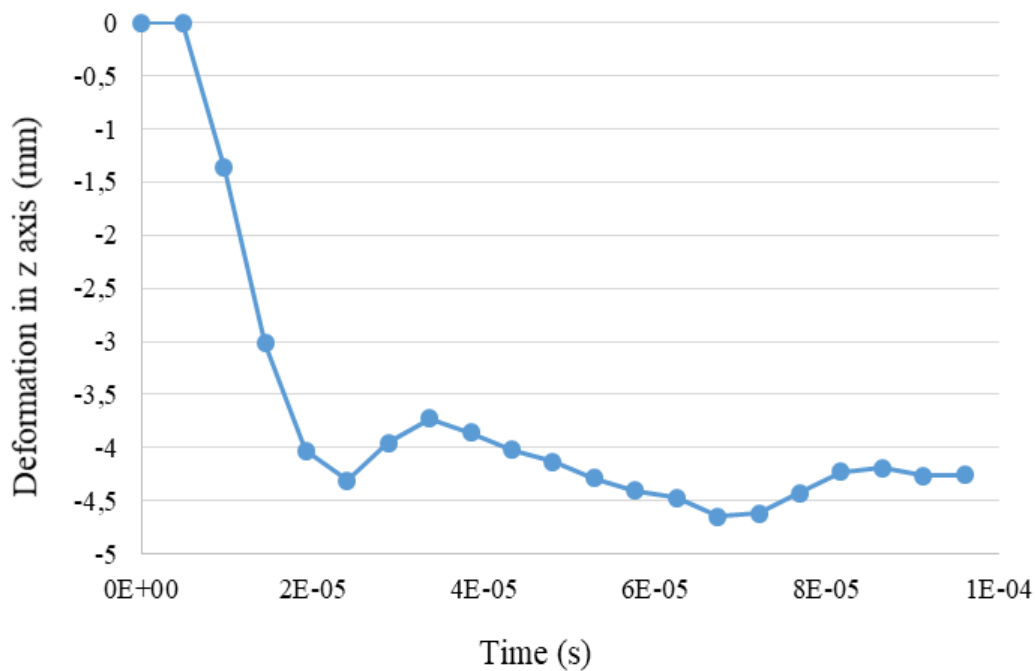
**Figure 3.34 :** Central deflection of the bottom layer of 23 layered Kevlar 29/epoxy – UHMWPE rectangular plate impacted by 300 m/s velocity of flat nosed Steel 4340 projectile.

## 3.9 Equivalent Stress Analyses for Different Impact Cases

Equivalent stress analyses are done for different high velocity impact scenarios. The importance of stress analysis is about determining critical area locations on a loaded body and prevent any failure of the considering system. Three different scenarios are investigated with the impact velocity of 300 m/s and the results are presented in Table 3.16. Illustrations of each of these stress analyses are shown in Figures 3.35 – 3.37.

**Table 3.16 :** Comparison of equivalent stresses for different impact scenarios.

| 300 m/s impact scenario | Maximum values of equivalent stress (MPa) |
|---|---|
| 19 layers of Kevlar 29/epoxy rectangular plate impacted by flat nosed projectile | 766,91 |
| 23 layers of Kevlar 29/epoxy – UHMWPE rectangular plate impacted by flat nosed projectile | 1151,10 |
| 23 layers of Kevlar 29/epoxy – UHMWPE rectangular plate impacted by conical nosed projectile | 1145,70 |
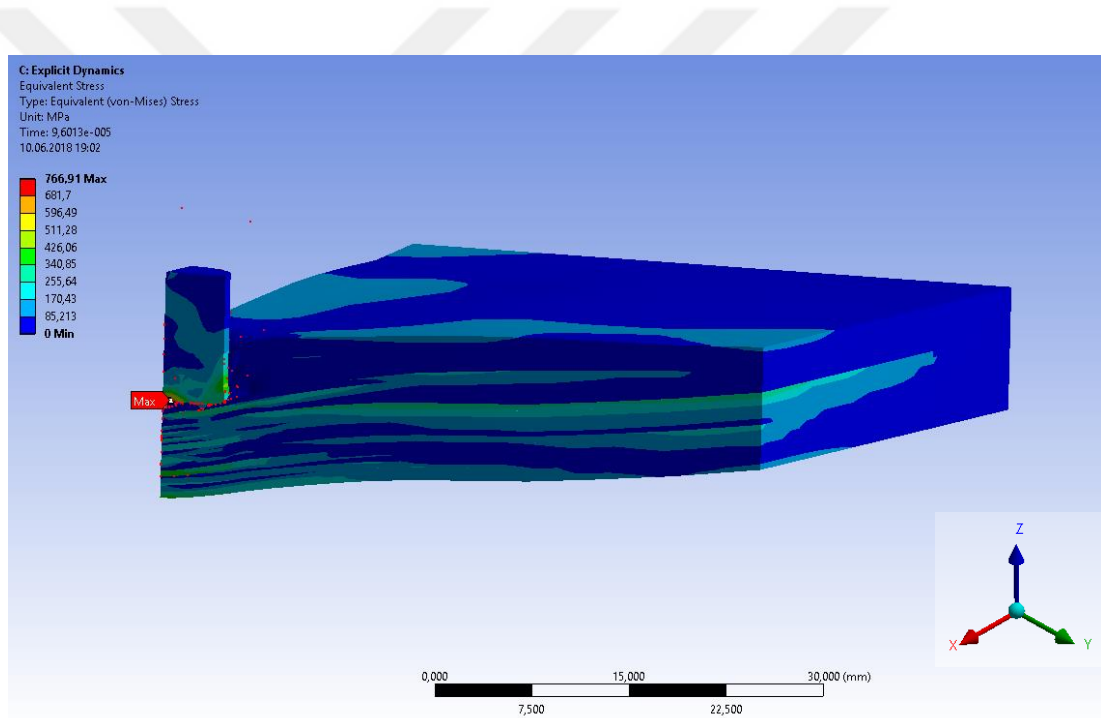


**Figure 3.35 :** Maximum equivalent stress analysis of 19 layers of Kevlar 29/epoxy rectangular plate impacted by flat nosed projectile.
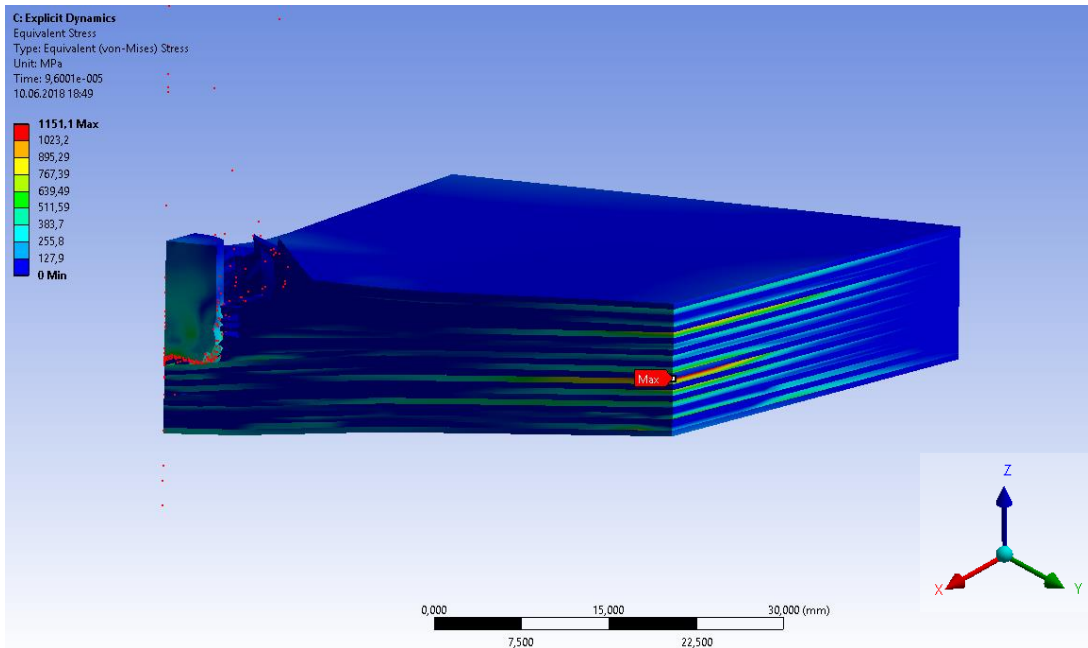
**Figure 3.36 :** Maximum equivalent stress analysis of 23 layers of Kevlar 29/epoxy – UHMWPE rectangular plate impacted by flat nosed projectile.
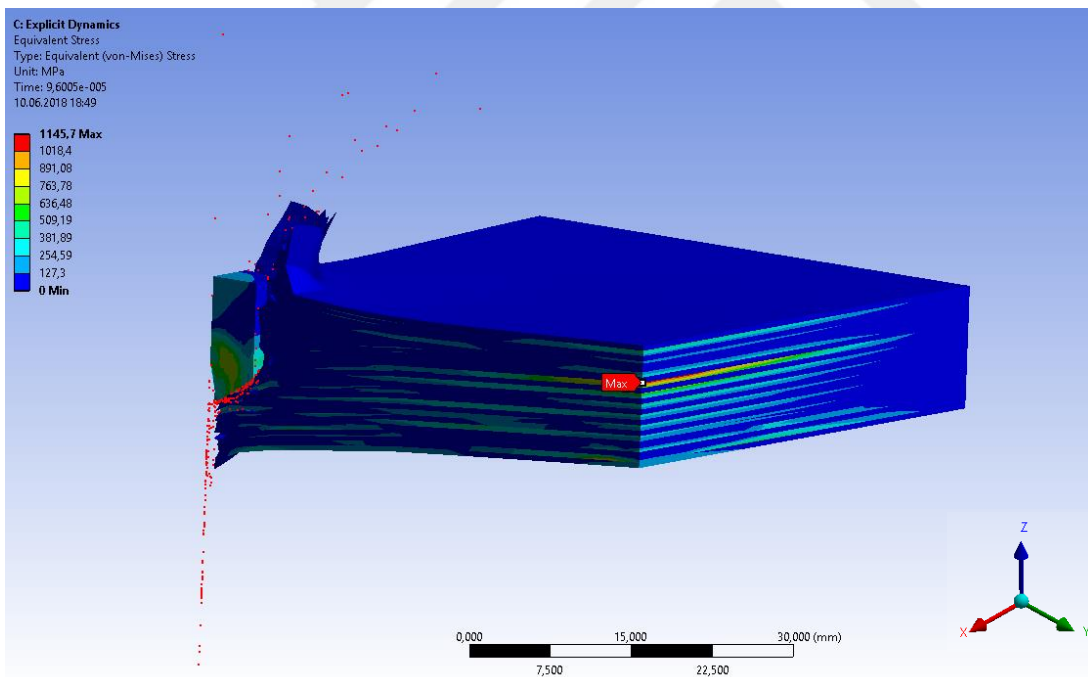


**Figure 3.37 :** Maximum equivalent stress analysis of 23 layers of Kevlar 29/epoxy – UHMWPE rectangular plate impacted by conical nosed projectile.

According to the analyses, maximum equivalent stress occurs on the plate area where the projectile impacted for 19 layers of Kevlar 29/epoxy rectangular plate impacted by flat nosed projectile; in between 13th and 14th layers from top and at the corner for 23

54

layers of Kevlar 29/epoxy – UHMWPE rectangular plate impacted by flat nosed projectile; and in between 7th and 8th layers from top and at the corner for 23 layers of Kevlar 29/epoxy – UHMWPE rectangular plate impacted by conical nosed projectile.

It can be concluded that for 300 m/s of impact velocity of Steel 4340 projectile, maximum equivalent stress occurs on the trajectory part of the plate for pure Kevlar 29/epoxy plates. On the other hand, for Kevlar 29/epoxy – UHMWPE plates, maximum equivalent stress occurs in between the layers and focused at one corner of the plate.

## 4. CONCLUSIONS

High-velocity impact response of Kevlar 29/epoxy – UHMWPE composite plate is investigated by FE method using ANSYS/AUTODYN simulation software. A FE model of a rectangular plate, with all-clamped boundary conditions and impacted by a flat nosed projectile made of Steel 4340, is developed. This model is verified by comparing the results with those in the literature. A relevant analysis showed that one quarter of the plate model can be used with sufficient accuracy for the sake of decreasing analysis time and system requirements. 5 different materials are compared with Kevlar 29/epoxy woven layer and with each other in terms of unit layers and the results of this comparison are presented. As a result, considering the unit layer weight and absorbed kinetic energy of the projectile, UHMWPE performs best with Kevlar 29/epoxy woven layers. For the stacking sequence arrangement, 4 different arrangements are tested. The results show that the stacking sequence in which UHMWPE layers placed in between Kevlar 29/epoxy layers one by one, decelerates the residual velocity of the projectile better than the other arrangements. For a unit plate area (100 mm × 100 mm), the final model ($[(K/U)_{11}/K]$) is 4,4 g lighter and slows down the projectile by 9,187% better than the 19 layers of Kevlar 29/epoxy model. The only drawback of the new model is the number of layers; Kevlar 29/epoxy – UHMWPE plate has 23 layers while its competitor has 19 layers – the difference in total thickness is 2 mm. The response of the composite plate to different high velocity impacts is analysed; the kinetic energy absorption of the composite plate and residual velocities of the projectile are presented.

Effect of projectile type is investigated by comparing high velocity impact test results of rectangular shaped Kevlar 29/epoxy - UHMWPE plate impacted by flat nosed and conical nosed Steel 4340 projectiles. The tests show that the average percentage of kinetic energy absorption of Kevlar 29/epoxy - UHMWPE plate impacted by flat nosed projectile is 62,81%. For the case with conical nosed projectile, the average percentage of kinetic energy absorption of the plate is 51,96%. By these results, it is shown that the percentage of kinetic energy absorption of target plate remarkably depends on the shape of projectile and Kevlar 29/epoxy - UHMWPE plate absorbs more kinetic

energy when it is impacted by a flat nosed projectile than it is impacted by a conical nosed projectile.

Effect of target plate shape is investigated by comparing high velocity impact test results of rectangular and circular shaped Kevlar 29/epoxy plates impacted by flat nosed Steel 4340 projectile. The tests show that the average percentage of kinetic energy absorption of rectangular shaped Kevlar 29/epoxy plate is 71,81% while the average percentage of kinetic energy absorption of circular shaped Kevlar 29/epoxy plate is 56,71%. According to these results, it is obvious that the percentage of kinetic energy absorption by the target plate remarkably depends on the shape of target plate and rectangular shaped Kevlar 29/epoxy plate absorbs more kinetic energy of impact than circular shaped one.

Investigations on the effect of impact obliquity on Kevlar 29/epoxy - UHMWPE plate impacted by 9 mm FMJ projectile show that the percentage of kinetic energy recoiled by the target plate depends on the angle of impact and despite the uncertainty between the results for 60° and 75° impacts, it can be said that percentage of kinetic energy recoiled by the plate increases while impact angle between projectile and target plate decreases.

The highlights of the findings are:

- After the stress analysis, considering the analysis time and approximation of results, it is concluded that one quarter model gives the optimum result with an error percentage of 7,06% and at 14,84% of the analysis time of the full model.

- Investigation of material type effects on high velocity impact loading indicates that heavier plates do not necessarily provide higher protection against high velocity impacts.

- Combined with UHMWPE, Kevlar 29/epoxy shows better ballistic performance than other ballistic materials considering layer weight and kinetic energy absorption.

- Layer stacking sequence tests indicate that, the sequence of 9 UHMWPE woven layers placed in between 10 layers of Kevlar-29/epoxy is the most effective sequence among all of the considered stacking sequences.

- 23 layers of Kevlar/epoxy - UHMWPE plate is lighter and more successful at decelerating the projectile velocity than 19 layers of Kevlar/epoxy plate. It is 2,81% lighter in weight and 9,19% better at decelerating the projectile velocity.

- It is determined that the percentage of kinetic energy absorption of target plate remarkably depends on shape of the projectile. 38,34% more kinetic energy of the flat nosed projectile is absorbed by the plate than of the conical nosed projectile.

- The rectangular plate absorbs 21,02% more kinetic energy of the projectile than the circular plate.

- Impact obliquity study indicates that as the impact angle between the trajectory and the plate increases, the plate recoils the projectile less effectively and experiences greater failure.

For the future studies, it is recommended to analyse other types of materials like ceramics and glass fibers as primary and/or secondary materials in bulletproof composite plates.

# REFERENCES

[1] **Varas, D., Artero-Guerrero, J. A., Pernas-Sánchez, J., López-Puente, J.** (2013). Analysis of high velocity impacts of steel cylinders on thin carbon/epoxy woven laminates. Composite Structures, 95, 623-629. doi:10.1016/j.compstruct.2012.08.015

[2] **Zhang, W., He, L., Li, P., Ye, Y., Feng, X., Novikov, L. S.** (2015). Dynamic response and numerical simulation of Al−Sc and Al−Ti alloys under high-speed impact. Transactions of Nonferrous Metals Society of China, 25, 559-570. doi:10.1016/S1003-6326(15)63638-X

[3] **Mohotti, D., Ngo, T., Raman, S. N., Mendis, P.** (2015). Analytical and numerical investigation of polyurea layered aluminium plates subjected to high velocity projectile impact, Materials and Design, 82, 1-17. doi:10.1016/j.matdes.2015.05.036

[4] **Park Y., Kim, Y., Baluch, A. H., Kim, C.** (2015). Numerical simulation and empirical comparison of the high velocity impact of STF impregnated Kevlar fabric using friction effects. Composite Structures, 125, 520-529. doi:10.1016/j.compstruct.2015.02.041

[5] **López-Puente, J., Zaera, R., Navarro, C.** (2003). High energy impact on woven laminates, Journal de Physique IV, 110, 639-644. doi:10.1016/j.compositesa.2007.10.004

[6] **López-Puente, J., Zaera, R., Navarro, C.** (2008). Experimental and numerical analysis of normal and oblique ballistic impacts on thin carbon/epoxy woven laminates. Composites: Part A, 39, 374-387. doi:10.1051/jp4:20030765

[7] **Bland, P. W., Dear, J. P.** (2001). Observations on the impact behavior of carbon-fibre reinforced polymers for the qualitative validation of models, Composites: Part A, 32, 1217-1227. doi:10.1016/S1359-835X(01)00076-8

[8] **Hammond, R. I., Proud, W. G., Goldrein, H. T. Field, J. E.** (2004). High-resolution optical study of the impact of carbon-fibre reinforced polymers with different lay-ups. International Journal of Impact Engineering, 30, 69-86. doi:10.1016/S0734-743X(03)00056-3

[9] **Hosur, M. V., Vaidya, U. K., Ulven, C., Jeelani, S.** (2004). Performance of stitched/unstitched woven carbon/epoxy composites under high velocity impact loading. Composite Structures, 64, 455-466. doi:10.1016/j.compstruct.2003.09.046

[10] **Kim, H., Welch, D. A., Kedward, K. T.** (2003). Experimental investigation of high velocity ice impacts on woven carbon/epoxy composite panels. Composites: Part A, 34, 25-41. doi:10.1016/S1359-835X(02)00258-0

[11] **Cantwell, W. J., Morton, J.** (1989). Comparison of the low and high velocity impact response of CFRP. Composites, 20, 545-551. doi:10.1016/0010-4361(89)90913-0

[12] **Will, M. A., Franz, T., Nurick, G. N.** (2002). The effect of laminate stacking sequence of CFRP filament wound tubes subjected to projectile impact. Composite Structures, 58, 259-270. doi:10.1016/S0263-8223(02)00050-8

**[13] Tham, C. Y., Tan, V. B. C., Lee, H. P.** (2008). Ballistic impact of a Kevlar helmet: Experiment and simulations. International Journal of Impact Engineering, 35, 304-318. doi:10.1016/j.ijimpeng.2007.03.008

**[14] Garcia-Avila, M., Portanova, M., Rabiei, A.** (2015). Ballistic performance of composite metal foams. Composite Structures, 125, 202-211. doi:10.1016/j.compstruct.2015.01.031

**[15] Min, S., Chen, X., Chai, Y., Lowe, E.** (2016). Effect of reinforcement continuity on the ballistic performance of composites reinforced with multiply plain weave fabric. Composites Part B, 90, 30-36. doi:10.1016/j.compositesb.2015.12.001

**[16] Wicklein, M., Ryan, S., White, D.M., Clegg, R.A.** (2008). Hypervelocity impact on CFRP: Testing, material modelling, and numerical simulation. International Journal of Impact Engineering, 35, 1861-1869. doi:10.1016/j.ijimpeng.2008.07.015

**[17] Zhou, Y., Chen, X.** (2015). A numerical investigation into the influence of fabric construction on ballistic performance. Composites Part B, 76, 209-217. doi:10.1016/j.compositesb.2015.02.008

**[18] Rizov, V.I.** (2007). Low velocity localized impact study of cellular foams. Materials and Design, 28, 2632-2640. doi:10.1016/j.matdes.2006.09.023

**[19] Toqueboeuf, B., Mortaigne, B., Cottenot, C.** (1997). Dynamic Behaviour of Polycarbonate/Polyurethane Multi-Layer for Transparent Armor. J. PHYS IV, C3, 499-504. doi:10.1051/j.jp4:1997386

**[20] Deka, L.J., Bartus, S.D., Vaidya, U.K.** (2009). Multi-site impact response of S2-glass/epoxy composite laminates. Composites Science and Technology, 69, 725-735. doi:10.1016/j.compscitech.2008.03.002

**[21] Ansari, M. M., Chakrabarti, A.** (2016). Impact behavior of FRP composite plate under low to hyper velocity impact. Composites Part B, 95, 462-474. doi:10.1016/j.compositesb.2016.04.021

**[22] Johnson, G. R., Cook, W. H.** (1985). Fracture characteristics of three metals subjected to various strains, strain rates, temperatures and pressures. Engineering Fracture Mechanics, 21, 31-48. doi:10.1016/0013-7944(85)90052-9

**[23] Johnson, G. R., Cook, W. H.** (1983). A constitutive model and data for metals subjected to large strains, high strain rates and high temperatures. *Proceedings of the 7th International Symposium on Ballistics* (pp. 541-547). The Hague, The Netherlands.

**[24]** Retrieved from https://www.sharcnet.ca/Software/Ansys/16.2.3/en-us/help/ans_elem/Hlp_E_PLANE182.html

**[25]** Retrieved from https://www.sharcnet.ca/Software/Ansys/16.2.3/en-us/help/ans_elem/Hlp_E_PLANE183.html

**[26]** Retrieved from https://cfd.ninja/bias-factor/

**[27] Liu, W., Chen, Z., Chen, Z., Cheng, X., Wang, Y., Chen, X., Liu, J., Li, B., Wang, S.** (2015). Influence of different back laminate layers on ballistic performance of ceramic composite armor. Materials and Design, 87, 421-427. doi:10.1016/j.matdes.2015.08.024

**[28] American National Standards Institute, Sporting Arms and Ammunition Manufacturers' Institute, Inc.** (2015). American National Standard Voluntary Industry Performance Standards for Pressure and Velocity of

Centerfire Pistol and Revolver Ammunition for the Use of Commercial Manufacturers. (ANSI/SAAMI Z299.3) Retrieved from http://www.saami.org/specifications_and_information/index.cfm?page=ANSI

[29] Retrieved from https://www.azom.com/article.aspx?ArticleID=1630

**CURRICULUM VITAE**

Latif Tibet Aktaş was born in Karacabey - Bursa, in 1991. He received B.Sc. degree in Mechanical Engineering from Dokuz Eylul University in 2016. He started M.Sc. in Mechanical Engineering Department - Engineering Mechanics in Izmir Katip Celebi University in the same year. He is working as a research assistant in Izmir University of Economics since 2017. His research interests include composite materials, finite element method and ballistic behavior of materials.

**List of Publications:**

**Conference Papers**

- **Aktaş, L. T.** (2017). The Effect of Air Bubbles in Matrix Phase and Environmental Temperature to Tensile Strength of E Glass – Epoxy Composites. *Proceedings of the International Students Science Congress*, İzmir, Turkey. Retrieved from http://sciencecon.org/archives/2017-2/
- **Aktaş, L. T., Çevik, M.** (2018). Finite Element Analysis of Material and Parameter Effects in Ballistic Armors. *Proceedings of the International Students Science Congress*, İzmir, Turkey. Retrieved from http://www.sciencecon.org

**Journal Papers**

- **Aktaş, L. T., Çevik, M.** (2018). Finite Element Analysis of Material and Parameter Effects in Ballistic Armors. Uludağ University Journal of The Faculty of Engineering – Under Consideration